Hindlimb Myology and Muscle Architecture in three-toed sloths (Xenarthra: Pilosa)

by

Dakota M. D. Morgan

Submitted in Partial Fulfillment of the Requirements

for the Degree of

Master of Science

in the

Biological Sciences

Program

YOUNGSTOWN STATE UNIVERSITY

August, 2021

Hindlimb Myology and Muscle Architecture in three-toed sloths (Xenarthra: Pilosa)

Dakota M. Morgan

I hereby release this thesis to the public. I understand that this thesis will be made available from the OhioLINK ETD Center and the Maag Library Circulation Desk for public access. I also authorize the University of other individuals to make copies of this thesis as needed for scholarly research.

Signature:

Dakota M. Morgan, Student	Date

Approvals:

Prof. Michael T. Butcher, Thesis Advisor	Date
Prof. Thomas P. Diggins, Committee Member	Date
Prof. Kenneth Learman, Committee Member	Date
Dr. Salvatore A. Sanders, Dean, College of Graduate Studies	Date

ABSTRACT

Tree sloths evolved below-branch locomotion making them one of few mammalian taxa beyond primates for which suspension is nearly obligatory. Suspension requires strong limb flexor muscles that provide both support and propulsion, and available locomotor mechanics data indicate that these roles differ between fore- and hindlimb pairs. Muscle structure in the pelvic limb is hypothesized to be a key anatomical correlate of functional roles in braking/support during suspensory walking and propulsion/support during vertical climbing. This expectation was tested by quantifying architecture properties in the hindlimb musculature of brown-throated three-toed sloths (***Bradypus variegatus***: N=7) to distinguish the roles of the flexor/extensor functional muscle groups at each joint. Measurements of muscle moment arm (r_m), muscle mass (MM), muscle length (ML), fascicle length (L_F), pennation angle (θ), and physiological cross-sectional area (PCSA) were taken from n=46 muscles. Overall, most muscles studied show properties for contractile excursion and fast joint rotational velocity. However, the flexor musculature is more massive (p=0.048) and has larger PCSA (p=0.003) than the extensors, especially at the knee joint and digits where well-developed and strong flexors are capable of applying large joint torque. Moreover, selected hip flexors/extensors and knee flexors have modified long r_m that can amplify joint torque in muscles with otherwise long, parallel fascicles, and one muscle (m. iliopsoas) was capable of moderately high power. The architectural properties observed for the hip flexors and extensors match well with roles in suspensory braking and vertical propulsion, respectively, whereas strong knee flexors and digital flexors appear to be main the muscles providing suspensory stability in the pelvic limb. With aid in support by the forelimbs and use of adaptive locomotor and muscle recruitments patterns, structure-function in the tensile limb systems of sloths collectively represents a mechanism for energy conservation.

ACKNOWLEDEMENTS

I sincerely thank my graduate advisor, Dr. Michael Butcher, for his guidance, patience, and mentoring throughout my Thesis research project and Masters Degree. I thank my graduate committee members, Drs. Thomas Diggins and Ken Learman, for their critical reviews of my Thesis, manuscript, and helpful comments. I am especially thankful for Dr. Diggins and his help with statistics. I am very grateful to Ms. Judy Avey-Arroyo for giving me access to frozen sloth specimens and for opportunity to interact with live sloths during the duration of collecting myological data for my Thesis at The Sloth Sanctuary of Costa Rica. I also thank Vincent Village for providing initial instruction with Adobe Illustrator. Last, I am grateful to my lab mates (former and present) Angela Mossor, Jordan Fain, Dragan Juzbasich, Michael Deak, and A.J. McKamy, who gave me consistent support throughout my tenure at YSU. Support for this research was provided by a Journal of Experimental Biology Traveling Fellowship [JEBTF2003440]. The YSU Office of Research and Department of Chemical and Biological Sciences are additionally acknowledged for their support. Finally, a Cushwa/Commercial Shearing Fellowship award funded my graduate assistantship AY 2020–2021.

DEDICATION

I dedicate this Thesis to my family: Mom, Dad, Nana, Papa, Ryleigh, and Aiden who taught me the values of dedication and persistence, and who have always given their love and encouragement. Without the collective support of my family, I would have given up and never been able to complete this Thesis.

TABLE OF CONTENTS

LIST OF TABLES

LIST OF FIGURES

INTRODUCTION

Tree sloths evolved below-branch (anti-pronograde) locomotion making them one of few mammalian taxa beyond primates for which suspension is nearly obligatory. Suspensory primates, however, may use pendulum-like exchanges of energy via arm swinging to reduce the metabolic cost of locomotion (Bertram and Chang, 2001), whereas such mechanics are not available to sloths. Instead, sloths must move in a slow, deliberate manner that minimizes fluctuations of the dynamic forces exerted on the substrate (Nyakatura and Andrada, 2013) so as not to make the support unstable, or oscillate, thus avoiding wasted effort when suspensory walking (SW). This suggests that their movements are entirely driven by muscle activation and positive work (Gorvet et al., 2020), or further that co-contraction of fore- and hindlimb flexors may be required to might make the long axis of the body rigid to prevent horizontal levering during SW (Granatosky et al., 2018). Moreover, since locomotion and posture in sloths is in the inverse orientation relative to pronograde mammals, gravitational induced extensor torques at the limb joints must be controlled by limb flexor muscles (Fujiwara et al., 2011). Muscle activations have been shown to be protracted and maximal for the elbow flexors when three-toed sloths performed suspensory locomotion (Gorvet et al., 2020). An anti-gravity role at the elbow joint has likewise been demonstrated for brachiating primates and in lorisids that employ suspensory locomotion as well as slow, intermittent movement patterns (Jungers and Stern 1980, 1981; Jouffroy and Stern, 1990).

Records of substrate reaction forces (SRF) are equally important to understanding tensile limb system function in arboreal taxa. In contrast to the patterns typical of primates, which show hindlimb-biased body weight support as well as net propulsive impulse by the hindlimbs (Hanna et al., 2017), Granatosky and Schmitt (2017) found that forelimbs of two-toed sloths are the main propulsion elements during SW, while the hindlimbs perform greater net braking, all while sloths maintain the position of their center of mass (CoM) evenly between their fore- and hindlimb pairs. These unusual locomotor mechanics are not fully understood or have yet to be studied in any species of *Bradypus*, whereas SRF are not available for vertical climbing (VC) in sloths. During VC, both pairs of limbs are expected to have a propulsive and support function similar to lorisids (Hanna et al., 2017). Given the overall similarity in behavior between the slow

loris (*Nycticebus*) and sloths, it is likely that the hindlimbs have an important anti-gravity role to play when grasping/clinging or climbing in an upright position. Therefore, in addition to SW in sloths, VC comes with an elevated energy expense (Hanna et al., 2008). Although, evidence from Gorvet et al. (2020) indicates that sloths may have the ability to offset some of the metabolic cost of both behaviors by selective recruitment of slow-contracting fibers when greater force production is required by their limb muscles.

The energetic cost of locomotion is largely dependent on the cost of muscle force production (Kram and Taylor, 1990), which in turn is determined by myosin heavy chain (MHC) expression and intrinsic fiber contractile properties. MHC fiber type and muscle metabolic characteristics are established for sloths. The myosin fiber type distribution in the limb musculature of three-toed sloths is nearly 90% slow MHC-1 (Spainhower et al., 2021). In particular, *Bradypus* expressed large proportions of slow MHC-1 fibers in their hip flexors implying a possible functional role of joint stability (i.e., anti-gravity muscles). Slow-contracting muscles are important for posture, in addition to controlling accelerations of the CoM (i.e., minimizing destabilization of the body). Both *Bradypus* and *Choloepus* also lack expression of the fast MHC-2X and -2B isoforms (Spainhower et al., 2018, 2021). Strong, slow-contracting muscle fibers could be a functional requirement for suspensory habits where sustained activations of numerous limb flexor muscles are expected to be necessary for joint stabilization and the prolonged gripping/grasping behaviors in sloths. However, beyond intrinsic contractile properties, muscle function is often constrained by fiber architecture (Lieber, 2009).

There are two main fiber architectures observed skeletal muscles: pennate- and parallel-fibered muscles. In general, pennate-fibered muscles have resting pennation angles of 15–45°, whereas parallel-fibered muscles have long fascicles that may approximate the length of the muscle belly and are orientated at low angles (0–15°) to the force axis of the muscle (Zajac, 1989, 1992). Muscles with pennate fascicles typically have large physiological cross-sectional area (PCSA) as well as the capacity for large isometric force production (Alexander, 1984; Williams et al., 2008). On the other hand, fascicles that are arranged in parallel to the line of action provide shortening ability (i.e., contractile excursion) and a greater capacity for performing work and power than pennate-fibered muscles (Gans, 1982, Azizi et al., 2008). Parallel-fibered muscles with

long fascicles are thus better suited for movements requiring velocity of contraction and/or large ROM at the limb joints. Indeed, the hindlimb of *Bradypus* was previously observed to contain predominantly parallel-fibered muscles (Butcher et al., in review); however, muscle architectural properties from the pelvic limb have not been examined for either genus of tree sloth, although they are available for the forelimb musculature (Diniz et al., 2018; Olson et al., 2018). To summarize, the forelimb of *Bradypus* demonstrates a proximal-to-distal increase in pennation, contains strong flexors, and has muscle gearings consistent with propulsion during both SW and VC, in addition to a common function of the musculature in suspensory support (Olson et al., 2018). Muscle properties related to joint stability should similarly be expected in the hindlimb, which may have an even greater role in support (Goffart, 1971), but its muscles should also be required to supplement work and power for VC.

This study aims to quantify muscle architectural properties in the hindlimb of the brown-throated three-toed sloth (*Bradypus variegatus*). Quantifications of fascicle length, PCSA, and muscle moment arm will help to distinguish the role of functional muscle groups, in addition to that of the hindlimb during arboreal locomotor behaviors in sloths. To this end, the contributions of the muscle mass and PCSA to force and torque application capacity will be used to further evaluate function in a tensile limb system. It is hypothesized that the architectural properties observed will be key anatomical correlates of functional roles in braking/support during SW and propulsion/support during VC. Specifically, for the hindlimb of *B. variegatus* it is predicted that: (1) total PCSA and summed torques (i.e., strength) of the flexor musculature will be larger than those of the extensors at the hip, knee, and ankle joints; (2) m. sartorius, m. iliopsoas, and/or m. adductor will have large PCSA and leverage at the hip joint for braking function during SW; (3) well-developed and strong knee flexors will have long muscle moment arms for the application of large medially-directed forces on the substrate to stabilize hindlimb support; and (4) hip extensors will have long fascicles, but appreciable muscle mass and moment arms for propulsion during vertical climbing. These expected results will substantially improve understanding of suspensory adaptations in sloth limbs.

MATERIALS AND METHODS

Study animals

The hindlimbs of *N*=7 three-toed sloths were previously dissected for this study (morphometric data available in Butcher et al., in review: Table 1). All individuals either died of natural causes or were euthanized for reasons unrelated to this study, and after which, were frozen (-20ºC) and stored until observation. Specimens were allowed to thaw for 24–30 h prior to dissection. One hindlimb (right or left) was used for muscle architectural measurements and the other for muscle harvesting (see Spainhower et al., 2021). The carcasses were disposed of by burning following muscle sampling. This work was conducted at The Sloth Sanctuary in Penshurst-Límon, Costa Rica in Spring 2015 and Spring 2017-2019. All procedures complied with protocols approved by the Costa Rica Ministry of the Environment, Energy, and Technology (MINAE: R-033-2015 to R. Cliffe and R. Olson; R-008-2017 to M.T. Butcher) and adhered to the legal requirements of the United States.

Hindlimb myology

Myological descriptions for *B. variegatus* dissection followed those of Macalister (1869), Humphrey (1870), Mackintosh (1875b), and Windle and Parsons (1899). Muscle nomenclature closely adhered to the Nomina Anatomica Veterinaria (NAV: International Committee on Veterinary Gross Anatomical Nomenclature 2012). Synonyms of several muscles (e.g., m. plantaris and m. peroneus longus) are provided to facilitate comparisons with previous works on sloth myology. Muscle names and abbreviations are presented in Table 1. Briefly, the hindlimbs were skinned and all muscles were systematically dissected (excised proximal-to-distal) beginning with extrinsic muscles of the hindlimb. Each belly was identified, and its origin, insertion, and fiber architecture (verified by microdissection) were recorded (Table 1), along with estimations of its actions (Table 2). Muscles were periodically moistened with a saline solution to prevent desiccation during the dissection. If observation and measurement could not be concluded in one day, then the limb was wrapped in gauze soaked in saline and stored overnight in a refrigerator. Several photographs were taken for each muscle belly and at each level of dissection with an α-nex 5 digital camera (Sony, Japan) and these images were used to construct limb muscle maps and illustrations of muscle topography (Butcher et al., in review).

Architectural properties

Architectural properties were taken from each muscle following established methods (Moore et al., 2013; Rose et al., 2013; Rupert et al., 2015; Olson et al., 2018). Muscle moment arm (r_m) was measured *in situ* as the perpendicular distance between the muscle line of action and the estimated joint center of rotation (marked with dissection pins pushed through the joints); it indicates the mechanical/velocity advantage a MTU has to either flex or extend a joint. Specifically, r_m was measured three times with the hip, knee, and ankle joints at an angle of 90°. Following the removal of each muscle and all associated free tendons, wet muscle mass (MM) was recorded to the nearest 0.1 g using an electronic balance (Model: Scout-Pro; Ohaus, USA). Muscle length (ML) was measured to the nearest 0.01 mm with digital calipers (Model: CD-8 CSX; Mitutoyo, Japan). Fascicle length (L_F) was measured at n=5–10 random sites (depending on muscle size) within the muscle belly with digital calipers. Lastly, pennation angle (θ: in deg) was recorded (n=5–10) using a goniometer to measure the angle (to the nearest degree) between the fascicles and either the muscle long axis or internal tendon; muscles averaging <15° were generally considered to be parallel-fibered. With the exception of MM, when possible, each of these metrics were taken *in situ* with the limb joints at the neutral position.

Data analysis

PCSA was calculated with the equation: $(V/L_F) \times \cos \theta$, where V is muscle volume (MM divided by a muscle density of 1.06 g cm^{-3}: Mendez and Keyes, 1960), L_F is *mean* fascicle length, and θ is *mean* pennation angle. Pennation angle was used in the calculations of PSCA (in cm^2) to permit more accurate estimates of isometric force (Williams et al., 2008b). While PCSA is typically larger in pennate-fibered muscles, it is important to recognize that parallel-fibered muscles with large mass can also have large PCSA due to the use of volume (mass and volume are related by density) in its calculation. Isometric force (F_{max}) was determined by multiplying PCSA by a maximum isometric stress of 30 N cm^2 (Woledge et al., 1985; Medler, 2002). Maximal joint torque (at a joint angle of 90º) was simply calculated as $F_{max} \times r_m$. Instantaneous muscle power (P_{inst}) was calculated as $0.1(F_{max} \times V_{max})$ (Hill 1938), where V_{max} is maximum fiber shortening velocity. A size-specific value of 0.58 FL s^{-1} (fiber lengths per second) for a 4

kg adult *B. variegatus* (Olson et al., 2018) was predicted using published slack test data (at 12ºC: Toniolo et al., 2007) for slow MHC-1 fibers in mammals (the primary isoform in sloths: Spainhower et al., 2018, 2021). Accounting for a Q_{10} of 2–6 for V_{max} (Pate et al., 1994; Ranatunga, 1996), a value of 2.3 FL s^{-1} was determined near physiologic temperature (~34ºC) for sloths. Importantly, F_{max}, joint torque, P_{inst} are estimates and are used here to indicate functional capacity of muscles (Williams et al., 2007b; Rupert et al., 2015; Olson et al., 2018). Last, two size-scaled ratios were computed as architectural indices (AI): fascicle length to muscle length (L_F/ML) and fascicle length to muscle moment arm length (L_F/r_m) (Rupert et al., 2015). A L_F/ML ratio close to 1.0 indicates large shortening ability, or contractile excursion, instead of force due to long fascicles, while a L_F/r_m greater than 2–3 indicates greater joint excursion (ROM) per change in muscle fascicle length.

Statistics

Descriptive statistics for all raw linear measurements and calculations were reported as mean ± s.d. (standard deviation) unless otherwise specified. All absolute measurements (except pennation angle) were scaled to body mass (BM) to account for the range in body size among the individuals sampled (juvenile to adult: 1.01–4.5 kg). Data were specifically normalized mass assuming the null hypothesis of isometry (Alexander et al., 1981; Biewener, 2005; Payne et al., 2005); lengths were scaled to $BM^{0.33}$, areas to $BM^{0.67}$, and masses to $BM^{1.0}$. Estimates of F_{max} (in N), joint torque (in N.cm), and power (in W) were simply normalized by directly dividing by BM (Moore et al., 2013; Rose et al., 2013). Individual limb muscles were also categorized into major functional groups for portions of this analysis: hip flexors (limb protractors), hip extensors (limb retractors), limb ab/adductors, knee flexors/extensors, ankle flexors/extensors, digital flexors/extensors, and foot-limb pronators/supinators. Bi-articular muscles were placed in more than one functional group (Table 2).

Selected muscle architectural metrics were additionally grouped (pooled and averaged) for statistical testing of flexor vs. extensor functional groups at each limb joint. These data represent only adult individuals (N=5) and were absolute (not normalized) values of MM, L_F, r_m, and PCSA. MANOVA (in SPSS) was used to determine statistical differences between suites of experimental variables among both the functional groups

studied and joint of action. Significance by MANOVA was followed by a series of one-way ANOVAs where Tukey's *post-hoc* tests were used to determine all pairwise differences. Significance for all statistical tests was accepted at $p \leq 0.05$.

RESULTS

Limb PCSA distribution

The hindlimb of *B. variegatus* contains 46 muscles (counting each head of selected muscles separately) that were studied. Means (±s.d.) of PCSA for each muscle are reported in Table 3. Average total hindlimb PCSA for *B. variegatus* is 21.8±10.6 cm^2. Muscles are organized into functional groups based on their main actions and their PCSA percentage distribution for *B. variegatus* is shown in Figure 1. The flexors collectively account for 76.2% of total hindlimb PCSA, whereas the extensors account for only 36.2%. In particular, the digital flexors are the functional group with the largest relative PCSA, accounting for 26.6±7.4% of the total hindlimb PCSA, with the two heads of the m. flexores digitorum profundi (FDP) being the major contributors to its isometric force capacity. The numerous and massive knee flexors similarly account a substantial 22.8±3.3% of total PCSA for the hindlimb followed by the functional groups hip flexors (mean: 16.9±4.6%) and hip extensors (mean: 12.6±4.5%) (Fig. 1). In general, however, the relative PCSA for each the extensor functional groups are notably smaller than that of their limb flexor counterparts. The pronators (mean: 6.57±1.8%) and supinators (mean: 5.96±1.9%) have the smallest relative PCSA among all functional groups in the hindlimb of *B. variegatus* (Fig. 1).

Normalized architectural properties

Figure 2A demonstrates a functional space plot of size scaled PCSA and L_F. Only the m. iliopsoas (ILPS) resides in the high-power quadrant of the plot. In addition to FDP, the m. gluteus medius (GLM) are the two muscles that are capable of large force production, whereas numerous muscles capable of operating over a large contractile range, including mm. gracilis (GRC), m. semimembranosus (SM), and both the lateral (LG) and medial (MG) heads of m. gastrocnemius as notable extremes in this capacity. The majority of hindlimb muscles are generalized in their functional ability, although there is an apparent shift towards the right in the plot associated with larger fascicle lengths (Fig. 2A).

The capacity of the hindlimb muscles to apply large joint torque is demonstrated in Figure 2B. ILPS is again the sole muscle in the large joint torque quadrant of the plot as it has both a sizable PCSA and r_m. The longest r_m are associated with the m. sartorius (SRT) at the hip joint and m. biceps femoris short head (BFS), yet they have low relative PCSA which limits the flexor torque they apply. In contrast, the large force production capability of GLM and FDP is paired with short relative r_m. Most muscles of the hindlimb have both low-to-modest PCSA and muscle moment arm lengths (Fig. 2B). Last, the capacity for fast joint rotational velocity by the hindlimb muscles is demonstrated in Figure 2C. Muscles associated with contractile range, or power, have long relative r_m reside in torque modified area of the plot, whereas no muscles have both long fascicles and moment arm lengths. However, numerous are capable of fast joint rotational velocity such as all the distal ankle flexor/extensors and m. flexor digitorum superficialis (FDS), in addition the m. gluteus superficialis (GLS), m. adductor longus (ADDL), and m. semitendinosus (ST) at both the hip and knee joints (Fig. 2C).

Summed torque at each joint for both flexors and extensors is presented in Table 4. Overall, the flexor muscles in the hindlimb of *B. variegatus* have a much greater capacity to apply joint torque (per unit body mass) compared to the extensors, especially at the knee joint with values of 98.3 N.cm Kg^{-1} and 34.0 N.cm Kg^{-1}, respectively. However, while estimated total joint torque is most similar between the hip flexors and extensors, the ankle/digital flexors can together apply more than four times the joint torque of the extensors at these joints. The digital flexors alone have substantial summed joint torque capability with a value of 62.8 N.cm Kg^{-1}, which is notable given that the m. extensor digitorum brevis (EDB) is only extensor of the digits in the hindlimb, and for which no r_m data are available for comparison of torques with the flexors.

Figure 3 represents the shortening ability of the hindlimb musculature. L_F/ML ratios larger than 0.7 typically indicate the capacity of muscles to undergo substantial length changes proportional to contractile velocity. Nearly half of the muscles in the hindlimb of *B. variegatus* have L_F/ML greater than 0.7 with the m. obturator internus (OI: 0.88), m. tensor fascia latae (TFL: 0.84), and the MG (0.84) having the three largest ratios (Fig. 3). Moreover, there is no distinct trend of decreasing L_F and increased pennation from proximal-to-distal along the length of the hindlimb, and apart from the knee extensors

that all have low-to-intermediate L_F/ML ratios, the majority of muscles comprising each limb region have values above 0.6 (Fig. 3). The m. vastus lateralis (VL) and m. tibialis caudalis (TCD) have the absolute lowest ratios at 0.33 and 0.34, respectively (Fig. 3).

The capability of muscle force production per unit muscle mass is shown in Figure 4. No muscles of the hindlimb have an ability to produce substantial force as all PCSA/MM are less than 0.6 (only the mm. gemelli have ratios >0.5). Moreover, one-third of the muscles analyzed have a ratio less than 0.2, although none of these are muscles located in hip or intrinsic foot regions of the limb. In addition to selected femoral rotator/stabilizers, the uni-articular knee extensors have appreciable PCSA/MM ratios (range: 0.42–0.49), with that of VL being the largest. Several pronator/supinators of the hind foot have moderate values for PCSA/MM (Fig. 4). Most notably, the pronators mm. fibularis brevis (FB) and fibularis quartus (FQ) have ratios of 0.38 and 0.42, respectively, while the hindfoot supinators TCD and m. tibialis cranialis fibular head (TCN-f) show nearly equivalent PCSA/MM.

Figure 5 represents the ability of a muscle to rotate a joint (or distal limb segment). The majority of muscles in the hindlimb of *B. variegatus* have L_F/r_m ratios greater than 3.0 indicating a capacity of musculature to move the limb joints through a sizable range of motion. Moreover, nearly half of the muscles analyzed have values ≥ 4.0 (Fig. 5). The leg region of the hindlimb contains muscles with the overall largest L_F/r_m with MG (9.26), FDS (7.78), and m. tibialis cranialis tibial head (TCN-t: 7.48) having the three largest ratios. Relatively few muscles have low values for L_F/r_m ranging from 1.25–2.79 and these include TFL, m. quadratus femoris (QF), m. sartorius (SRT) at the hip joint, m. biceps femoris short head (BFS), m. vastus intermedius/medialis (VI-VM), FB, TCN-f, and m. quadratus plantae (QP). These muscles with increased mechanical advantage are distributed about each limb region, and with the exception of the knee extensors, are mainly flexor muscles (Fig. 5).

Flexor and extensor muscle architectural properties at each hindlimb joint are compared in Figure 6. Although not significant (p=0.997), the extensor muscles are absolutely more massive than the flexors at the hip joint, whereas average mass of the flexors at both the knee and ankle joints are larger than that of the extensors, but significant at only the knee (p=0.048) (Fig. 6A). Average mass of the ankle extensors is

the lowest among all functional groups analyzed. Flexor muscle moment arms are longer at the hip (p=0.010) and knee (p<0.001) joints compared with the ankle flexors. Average r_m of the flexors at the ankle joint are also shorter albeit not significant (p=0.329) compared to that of ankle extensors, which have the longest r_m among the extensor muscles. However, at only the knee joint are there significant differences (p=0.006) in r_m between flexors and extensors (Fig. 6B). On average, the knee flexors have longer fascicle lengths than the flexors at both the hip (p<0.001) and ankle (p=0.012) joints, but have similar L_F with the extensors acting at the same joints. The flexors at the knee joint are additionally the only muscles that have significantly longer fascicles (p<0.001) than their counterpart knee extensors (Fig. 6C). Average L_F of the ankle flexors is also longer (p=0.027) than that of the extensor muscles acting at the knee joint, which have the shortest L_F among all functional groups analyzed. Finally, total PCSA of the flexors is larger than that of the extensors at each limb joint, but only the differences at the knee are significant (p=0.003). Total PCSA for the knee flexors muscles is the absolute largest, followed by that of hip flexors/extensors, and then the flexors acting at the ankle joint. On average, total PCSA for the knee flexors is also significantly greater than that of both the ankle flexors (p=0.012) and extensors (p<0.001) (Fig. 6D).

DISCUSSION

Muscle architectural properties for the pelvic limb in three-toed sloths broadly reveal a capacity for limb joint excursion and rapid movements that belie their observed locomotor patterns. Indeed, sloths move slowly, emphasizing the application of sizable flexor moments for joint stability and body control (i.e., braking function) by the hindlimbs during suspensory walking (SW). Key findings for selected muscles and/or functional groups support this hypothesis, including large PCSA in the hip, knee, and digital flexor musculature, several hip/knee flexors and adductors that are modified with muscle long moment arms, and the ability to generate appreciable power in only one hip flexor muscle. Moreover, certain properties observed are complimentary to those found in analogous functional groups in the forelimb of *B. variegatus* (Olson et al., 2018), although in totality, the estimated functional capacity in the pelvic limb appears to oppose a role in propulsion by sloth forelimbs. Thus, the results reported herein offer additional

insight into integrative limb pair function for suspensory habits and correlate well with other muscle characteristics indicating the critical need for energy conservation in sloths.

The flexor muscles in the pelvic limb are relatively well-developed showing significantly more mass than those of the extensors at the knee and ankle joints, in particular. These flexors notably exhibit the capability of producing appreciable isometric force. Due to increased pennation in selected muscle bellies of the distal limb, the digital flexors account for the greatest percentage of PCSA, which could be required for strong and/or prolonged grip on the substrate. In taxa for which suspension is nearly obligatory, grip strength is important as is the ability of the digital flexors to sustain contraction for grasping-clinging in either inverted or vertical (e.g., climbing) postures. Sloths spend approximately 23% of their daily active time in suspensory postures, albeit the upper bound of this estimate is more representative of *Choloepus* than *Bradypus* (Urbani and Bosque, 2007). Nonetheless, sloths have several features that are expected to facilitate maintenance of a strong grip, including ***rete mirabile*** in their limbs (Wislocki, 1928), selective recruitment of small, fast motor units in their digital flexors at low levels of activation for postural suspension (Gorvet et al., 2020), and flexor tendon suspensory apparatus capable of substantial passive support of their body weight (Mossor et al., 2020). Specifically, sloths have thick, but pliant digital flexor tendons with elevated safety factors in the hindlimb compared with their forelimbs (Mossor et al., 2020) consistent with a potentially greater role in suspensory support by the pelvic limbs as previously suggested (Goffart, 1971). A passive means of support via tensile loading in combination with low levels of active muscle tension for support is the most likely means to conserve metabolic energy for routine suspension.

The size and strength of the knee flexors is considerable in the pelvic limb of ***B. variegatus,*** and this functional group may be the most important to total limb support. Granatosky and Schmitt (2017) showed that in addition to the hindlimbs performing greater net braking during SW, both limb pairs exerted considerable medial SRF. Much like what has been suggested about large activation of their strong elbow flexors (Gorvet et al., 2020), as predicted, the ability of the massive knee flexors to apply the greatest amount of joint torque (~100 N.cm kg^{-1}) may play an analogous role in producing sizable medial SRF and mitigating levels of limb loading at the hip joint. The application of a

large flexor moment results from not only large PCSA, but also elongated muscle moment arms at the knee joint as seen in both SM and BFL (Figs. 2C, 6B). These features combined should aid in the maintenance of postural suspension and stabilization during SW by the knee flexors, as well the limb adductors, directing force medially on the substrate (Granatosky et al., 2018). In general, locomotion in sloths is best matched with muscle architectural properties indicative of enhanced leverage to apply sizable flexor moments at each limb joint for slow, controlled movements. The hindlimb flexors are well suited for an anti-gravity role in this regard, as they cannot apply equivalently large flexor moments as the forelimb flexor musculature (Olson et al., 2018), which are used for propulsion, in addition to support. Moreover, the hindlimb extensors are only half as strong as their counterpart shoulder flexors, thus limiting their ability to apply joint torque for propulsion during SW, and sloths have been shown to favor hindlimb positions in protraction versus retraction (Granatosky et al., 2018). Arboreal primates, however, show greater flexor/extensor development in their pelvic limbs compared with sloths suggesting both antigravity and propulsory functions while in anti-pronograde postures (Demes, 1984; Jouffroy and Stern, 1990; Hanna et al., 2008).

Beyond a role in knee flexion, the bi-articular flexor SRT, in addition to the parallel-fibered ILPS and ADDM, also have elongated moment arms at the hip joint. Such a modification improves the ability to apply an appreciable flexor moment at the hip thereby slowing joint rotation. In turn, the torque applied by these three muscles could be used slow the horizontal translation of the center of mass (CoM). The muscle most likely to serve a braking function is the SRT via co-activation with the m. pectoralis superficialis in the forelimb to keep the CoM evenly distributed between the limb pairs as previously hypothesized (Gorvet et al., 2020). The SRT in *B. variegatus* expresses 100% slow-contracting fibers (Spainhower et al., 2021) and can produce force slowly that would be further enhanced in magnitude by undergoing a lengthening contraction as the body advances forward below the substrate. It is also likely that the powerful ILPS is synergistic in this function with SRT. Moreover, Gorvet et al. (2020) showed the *Bradypus* moves quite slowly (0.07 ms^{-1}) and thus has little need for large joint excursions except by their forelimbs when protracted to purchase the substrate for their next stride cycle. Though joint angles were not quantified in that study, joint kinematics

evaluated in the pelvic limb of *Choloepus* indicate a limited range of motion at each the hip, knee, and ankle joints (Granatosky et al., 2018). Specifically, two-toed sloths tend to keep their hip joint protracted, knee flexed, and foot supinated during suspensory posture, whereas the hip and knee are placed in more adducted and extended positions, respectively, during SW. Comparable kinematics (and SRF) data are not currently available for any species of *Bradypus*.

The ability to slow the velocity of joint rotation is an apparent modification for increasing the mechanical advantage of selected muscles in sloth limbs. Similarly, Olson et al. (2018) found several muscles in the forelimb with this form: a purported mismatch in muscle bellies having both long fascicles and moment arms for enhanced joint torque. Also found in that study were subsets of muscles within each region of the forelimb of *B. variegatus* that have properties for limb joint rotation/velocity, and others for joint stability. This arrangement of muscle functional groups with opposite properties was suggested to represent possible muscle gearing that facilitates the deliberate, controlled movements in sloths (Olson et al., 2018). Although similar muscle gearings were not clearly duplicated within functional groups in the pelvic limb, the overall consistency in slow myosin heavy chain (MHC-1) isoform expression (Spainhower et al., 2018, 2021) between fore- and hindlimb pairs underscores that by being extremely slow-contracting, the limb musculature favors force production at the expense of contractile velocity.

Nevertheless, much like the forelimb musculature in *B. variegatus*, numerous muscles indeed show elevated L_F/r_m (ratios >2–3) that correlate with a large joint range of motion and/or fast velocity of joint rotation. Most of these muscles are found within in thigh region and have intermediate L_F/r_m compared to other muscles of the limb. Very high values of L_F/r_m (range: 8–34) are more typically observed in muscles (e.g, GLS, TFL, SM, BFL) acting at the proximal limb joints in cursorial taxa such cats (Sacks and Roy, 1982), hares (Williams et al., 2007a), and dogs (Williams et al., 2008a); however, those of three-toed sloths do not exceed an L_F/r_m of 10, and except for GLS and GLM, the muscle with the greatest values for this architectural index act at the knee and ankle joints. Thus, as expected, *Bradypus* deviates from the cursorial pattern of a proximal-to-distal decrease in L_F/r_m by retaining relatively more parallel-fibered muscles throughout their pelvic limb, with numerous bellies in each functional group having long fascicles.

Most of muscles with elevated L_F/r_m also have large L_F/ML emphasizing the effect of long fascicles, yet several muscles at the hip (e.g., femoral rotators), knee, ankle, and digits show nearly equivalent, intermediate ratios of both L_F/ML and PCSA/MM. Therefore, despite having relatively long fascicles, these bellies retain appreciable force per unit mass capability and may act as strong joint stabilizers, especially if coupled with low values of L_F/r_m as are notably some distal limb muscles (e.g., POP, FDP, TCD, FB). Other muscles with comparatively higher values of L_F/r_m must then act primarily as joint rotators. For example, the observed marked supination of the hindfoot in *Bradypus* while in contact with the substrate (Mendel 1985; Gorvet et al., 2020) is largely performed by heads of the m. tibialis cranialis complex (e.g., TCN-f) (Butcher et al., in review) and must be counterbalanced by hindfoot pronators such as FB and FQ.

It is equally notable that ILPS has the morphology of long fascicles and a long moment arm, but it is the only muscle capable of appreciable power generation (Fig. 2A). Considering that the duty factor for *Bradypus* is 0.83 regardless of moving beneath or up the substrate (Gorvet et al., 2020), power generation in this well-developed hip flexor muscle might be necessary for advancing the pelvic limb (i.e., hip protraction) in preparation of the next step and/or for lifting (and maintaining) the body towards the substrate. The latter function may also allow the hip flexors to absorb the body weight of the animal as the ipsilateral forelimb releases its grip on the substrate to progress the stride cycle. Although not as powerful by their architectural properties (MHC fiber is not known for ILPS), GLM and FDS have the capacity for moderate power attributed to their large PCSA and appreciable fascicle lengths. These two muscles could use their power capacity along with their muscle gearing for extension of the hip and flexion of the knee, respectively, during locomotion. Nevertheless, despite having the extrinsic (this study) and intrinsic (Spainhower et al., 2021) capacities for more powerful joint movements, sloths must move in a slow, controlled manner to minimize the following: 1. oscillations of the substrate, 2. chances of being detected by a predator, and 3. metabolic cost of muscle contraction due to their energy poor diet and correlated low metabolic rate (Pauli et al., 2016).

One final aspect of locomotor behavior in sloths is vertical climbing (VC), which comes with a costly energy expense (Hanna et al., 2008). Consequently, sloths require a

means of overcoming the expenditure while propelling themselves up a substrate, and for *Bradypus*, this most likely involves enhanced limb mechanical advantage provided by a shortened tibia, long calcaneus, short metatarsals, and long recurved claws (Marshall et al., 2021). Nevertheless, the functional group most likely to provide vertical propulsion are the hip extensors due to their larger relative mass and PCSA against that of the hip flexors. Perhaps more impressive is that a substantial amount of the total PCSA for this functional group is attributed to the GLM, which is three fused muscles in most specimens, as well as the bi-articular SM. Furthermore, the hip extensors were the only functional group for which no measured architectural properties differed significantly from those of any flexor group. Interestingly, lorisids were previously shown to rely equally on their fore- and hindlimb pairs for support/propulsion during climbing in comparison to other arboreal primates that show more hindlimb dominant propulsion (Hanna et al., 2017). SRF data are not available for sloths during VC, but EMG activation timing and intensities from forelimb flexor/extensor muscle pairs suggest a major role in vertical support by the hindlimbs of *B. variegatus* (Gorvet et al., 2020), which agree with similar EMG data from the hindlimbs in the slow loris (*Nycticebus coucang*: Jouffroy and Stern, 1990). Future studies of EMG in the pelvic of *Bradypus* are needed to clarify activation patterns of both synergistic and antagonist muscle pairs for functions in propulsion or joint stabilization, respectively.

A last consideration is how might the roles of joint stabilization and propulsion by the extensor musculature be distributed along the pelvic limb in relation to VC. Appreciable fascicle lengths and muscle moment arms of the hip extensors suggest some vertical propulsion and an intermediate joint stabilizer function. However, analogous muscles in the forelimb (i.e., limb retractors-shoulder flexors) were found to have the capacity to apply a flexor moment that is over 4 times larger that of the hip extensors (Olson et al., 2018), leading to speculation the forelimbs are considerably stronger than the hindlimbs and are the main propulsive elements for locomotion in sloths. The pennate knee extensors (i.e., vastus heads) show the capability of marked force production, which is required to counterbalance large flexor moments applied at the knee joint. Thus, the knee extensors likely play a key role broadly in joint stabilization; a role that may additionally extend to the infrequent crawling mode of terrestrial locomotion observed in sloths.

Contractions of the distal ankle extensor muscles for support may also be aided by observed appreciable mechanical advantage at the ankle joint of *Bradypus* (Marshall et al., 2021). Beyond vertical support for prolonged VC, the ankle extensors could also supplement vertical propulsion. Three-toed sloths notably spend a large proportion of their active time climbing and will climb to the emergent level of the rainforest (Urbani and Bosque, 2007). The ability to apply a sizable extensor moment at the ankle, in addition to a fully supinated hindfoot in contact the substrate, would greatly benefit sustained vertical clinging; a strategy that should allowing sloths to conserve energy while climbing.

Concluding remarks

This analysis of muscle architectural properties in the pelvic limb of *B. variegatus* indicates several expected and unexpected features of the musculature. Despite the requirement of large flexor moments for suspensory support and slow, intermittent locomotion, many sloth limb muscles demonstrate long, parallel fascicles and short moment arms that are paired with overall reduced extensor muscle mass. In order to counteract the joint rotational velocity advantage indicated by this muscle form, sloths appear to have several modifications in their limbs, such as multiple flexor muscles (or functional groups) capable of applying large torque for joint stability by elongation of moment arms and strong digital flexors for maintenance of grip force. These properties should allow the muscles of sloths to perform slow, forceful contractions while operating with greater mechanical advantage to move their limb joints at lower velocity. Beyond an equal role in support, muscle architectural properties between the fore- and hindlimbs are well matched to their respective functions of propulsion and braking control. Moreover, the extensors of the pelvic limb are less suited to provide substantial vertical propulsion but may be essential to support for slow climbing and grasping-clinging behavior. In this regard, sloths are convergent with lorisid primates. Future studies aim to determine possible muscle co-activation patterns of recruitment in both synergistic and antagonist muscle pairs to further clarify functional roles in propulsion, joint stabilization, and braking function between limb pairs in three-toed sloths. This work to be coupled with novel recordings of substrate reaction forces in *Bradypus* will provide additional insight

into the mechanisms of tensile limb loading in suspensory taxa and equal weight-bearing support between limb pairs observed only in tree sloths.

REFERENCES

Alexander, R. M. (1984). Stride length and speed for adults, children, and fossil hominids. *Am. J. Phys. Anthropol.* 63, 23–27.

Alexander, R., Jayes, A. S., Maloiy, G. M. O. and Wathuta, E. M. (1981). Allometry of the leg muscles of mammals. *J. Zool.* 194, 539–552.

Azizi, E., Brainerd, E. and Roberts, T. J. (2008). Variable gearing in pennate muscles. *Proc. Nat. Acad. Sci.* 105: 1745–1750.

Barrat, E. S. (1965). EEG correlates of tonic immobility in the opossum (*Didelphis virginiana*). *Electro. Clin. Neuro.* 18: 709–711.

Bertram, J. E. A. and Chang, Y. H. (2001). Mechanical energy oscillations of two brachiation gaits: measurement and simulation. *Am. J. Phys. Anthropol.* 115: 319–326.

Biewener, A. A. (1998). Muscle-tendon stresses and elastic energy storage during locomotion in the horse. *Comp. Biochem. Physiol. Part B,* 120: 73–87. doi:10.1016/s0305-0491(98)00024-8

Biewener, A. A. (2005). Biomechanical consequences of scaling. *J. Exp. Biol.* 208: 1665–1676.

Bottinelli, R. (2001). Functional heterogeneity of mammalian single muscle fibres: Do myosin isoforms tell the whole story? *Pflügers Arch.* 443, 6–17.

Britton, S. W. and Atkinson, W. E. (1938). Poikilothermism in the sloth. *J. Mammal.* 19: 94–99.

Britton, S. W. (1941). Form and function in the sloth. *Q. Rev. Biol.* 16: 13–34.

Butcher, M. T., Morgan, D. M., Spainhower, K. B., Chadwell, B. A., Thomas, D. R., Kennedy, S. P., Avey-Arroyo, J. A. and Cliffe, R. N. Myology of the pelvic limb of the brown-throated three-toed sloth (*Bradypus variegatus*). In review, *J. Anat.*

Clarke, A. and Rothery, P. (2007). Scaling of body temperature in mammals and birds. *Func. Ecol.* 22, 58–67. 10.1111/j.1365-2435.2007.01341. x.

Cliffe, B. N., Haupt, R. J., Avey-Arroyo, J. A. and Wilson, R. P. (2015). Sloths like it hot: Ambient temperature modulates food intake in the brown-throated sloth (*Bradypus variegatus*). *PeerJ* 3: e875.

Cliffe, B. N., Scantlebury, M. D., Kennedy, S. J., Avey-Arroyo, J. A., Mindich, D. and Wilson R. P. (2018). The metabolic cost of the Bradypus sloth to temperature. *PeerJ* 6: e5600.

Cohen, A. H., and Gans, C. (1975). Muscle activity in rat locomotion: Movement analysis and electromyography of the flexors and extensors of the elbow. *J. Morphol.* 146, 177–196.

Enders, R. K. (1935). Mammalian life histories from Barro Colorado Island, Panama. *Bull. Mus. Comp. Zool*. 78, 383–502.

Fujiwara, S. I., Endo, H. and Hutchinson, J. R. (2011). Topsy-turvy locomotion: biomechanical specializations of the elbow in suspended quadrupeds reflect inverted gravitational constraints. *J. Anat.* 219: 176–191.

Gans, C. (1982). Fiber architecture and muscle function. *Exerc. Sport Sci. Rev*. 10, 160–207.

Gardner, A. L. (2005). Order Pilosa. In: Mammal species of the world: A taxonomic and geographic reference (eds. D. E. Wilson and D. M. Reeder) pp. 100–103. Baltimore: Johns Hopkins University Press.

Gardner, A. L. (2008). Mammals of South America, Vol. 1: Marsupials, Xenarthrans, Shrews, and Bats. Chicago: University of Chicago Press.

Garla, R. C., Setz, E. Z. F. and Gobbi, N. (2001). Jaguar (Panthera Onca) food Habits in Atlantic rain Forest of southeastern *Brazil Biotropica* 33: 691–696.

Gaudin, T. J. (2004). Phylogenetic relationships among sloths (Mammalia, Xenarthra, Tardigrada): The craniodental evidence. *Zool. J. Linn. Soc., Lond*. 140: 255–305.

Gaudin, T. J. and McDonald, H. G. (2008). Morphology-based investigations of the phylogenetic relationships among extant and fossil xenarthrans. In The biology of the

Xenarthra (eds. S. F. Vizcaíno and W. J. Loughry), pp. 24–36. Gainesville: University Press of Florida.

Gaudin, T. J. and Croft, D. A. (2015). Palogene xenarthra and the evolution of South American mammals. *J. Mammal*. 96: 622–634.

Genoways, H. H. and Timm, R. M. (2003). The Xenarthrans of Nicaragua. *J. Neotrop. Mamm*. 10: 231–253.

Gillespie, D. S. (2003). Xenarthra: Edentata. In Zoo and wild animal medicine (eds. M. E. Fower and E. Miller), pp. 397–407. Philadelphia: W.B. Saunders Company.

Granatosky, M. C., Fitzsimons, A., Zeininger, A. and Schmitt, D. (2018). Mechanisms for the functional differentiation of the propulsive and braking roles of the forelimbs and hindlimbs during quadrupedal walking in primates and felines. *J. Exp. Biol.* 221: 1–11.

Granatosky, M.C. and Schmitt, D. (2017). Forelimb and hind limb loading patterns during below branch quadrupedal locomotion in the two-toed sloth. *J. Zool.* 302: 271–278.

Grand, T. I. (1978). Adaptations of tissue and limb segments to facilitate moving and feeding in arboreal folivores. In The ecology of arboreal folivores (ed. G. G. Montgomery), pp. 231–241. Washington, DC: Smithsonian Institution Press.

Hanna, J. B, Granatosky, M. C., Rana, P. and Schmitt, D. (2017). The evolution of vertical climbing in primates: evidence from reaction forces. *J. Exp. Biol.* 220: 3039–3052.

Hanna, J. B., Schmitt, D. and Griffin, T. M. (2008). The energetic cost of climbing in primates. *Science* 320: 898.

Hayssen, V. (2010). *Bradypus variegatus* (Pilosa: Bradypodidae). *Mammal. Spec.* 42: 19–32.

Hayssen, V. (2011). *Choloepus hoffmanni* (Pilosa: Megalonychidae), *Mammal. Spec.* 43: 37–55.

Hermanson, J.W. and Cobb, M.A. (1992). Four forearm flexor muscles of the horse, *Equus caballus*: Anatomy and histochemistry. *J. Morphol*. 212: 269–280.

Hildebrand, M. (1960). How animals run. *Sci. Am.* 202: 148–157.

Hildebrand, M. (1985). Walking and running. (Hildebrand, M., Bramble, D. M., Liem, K. F., Wake, D. B. eds.), Functional Vertebrate Morphology, pp. 38–58. Harvard University Press, Cambridge.

Hill, A. V. (1938). The heat of shortening and the dynamic constants of muscle. *Proc. R. Soc. B.* 126: 136–195.

Hodson-Tole, E. F., Wakeling, J. M. and Dick, T. J. M. (2016). Passive muscle-tendon unit gearing is joint dependent in human medial gastrocnemius. *Front. Physiol*. 7: 1–8.

Humphrey, G. M. (1870). The myology of the limbs of the Unau, the Ai, the two-toed anteater, and the Pangolin. *J. Anat. Physiol*. 3: 2–78.

Jenkins, F. A. and Weijstouch, W. A. (1979). The functional anatomy of the shoulder in the Virginia opossum (*Didelphis virginiana*). *J. Zool. Lond.* 188: 379–410.

Jouffroy, F. K. and Medina, M. F. (2004). Comparative fiber-type composition and size in the antigravity muscles of primate limbs. In Shaping Primate Evolution Form, Function, and Behavior (eds. F. Anapol, R. Z. German, and N. G. Jablonski), pp. 134–161. Cambridge: Cambridge University Press.

Jouffroy, F. K. and Stern, J. T. (1990). Telemetered EMG study of the antigravity versus propulsive actions of knee and elbow muscles in the slow loris. In Gravity, posture and locomotion in primates (eds. F. K. Jouffroy, M. H. Stack, and C. Niemitz), pp. 221–236. Florence: Il Sedicesimo.

Jouffroy, F. K., Stern, J. T., Médina, M. F. and Larson, S. G. (1999). Functional and cytochemical characteristics of postural limb muscles of the rhesus monkey: a telemetered EMG and immunofluorescence study. *Folia Primatologica* 70: 235–253.

Jungers, W. L. and Stern, J. T. (1980). Telemetered electromyography of forelimb muscle chains in gibbons (*Hylobates lar*). *Science* 208: 617–619.

Jungers, W. L. and Stern, J. T. (1981). Preliminary electromyographical analysis of brachiation in gibbon and spider monkey. *Int. J. Primatol.* 2: 19–33.

Kohn, T. A., Hoffman L. C. and Myburgh, K. H. (2007). Identification of myosin heavy chain isoforms in skeletal muscle of four African ruminants. *Comp. Biochem. Phys. A.* 148: 399–407.

Kohn, T. A., Curry, J. W. and Noakes, T. D. (2011). Black wildebeest skeletal muscle exhibits high oxidative capacity and a high proportion of type IIx fibres. *J. Exp. Biol.* 214: 4041–4047.

Kohn, T.A. (2014). Insights into the skeletal muscle characteristics of three southern African antelope species. *Biol. Open* 3: 1037–1044. doi: 10.1242/bio.20149241

Kram, R. and Taylor, C. R. (1990). Energetics of running: a new perspective. *Nature* 346, 265–267.

Lieber, R. L. (2002). Skeletal muscle structure, function, and plasticity (ed. T. Julet). Baltimore: Lippincott Williams & Wilkins.

Lieber, R. L. (2009). Skeletal muscle, structure, function, and plasticity, 3rd ed. Baltimore: Lippincott Williams & Wilkins: 369.

Macalister, A. (1869). On the myology of *Bradypus tridactylus*; with remarks on the general muscular anatomy of the Edentata. *Trans. R. Irish Acad.* 25: 51–67.

Mackintosh, H. W. (1875). On the muscular anatomy of *Choloepus didactylus*. *Proc R Irish Acad. Sci.* 2: 66–79.

Mackintosh, H. W. (1875). On the Myology of the Genus Bradypus. *Proc. R. Irish Acad. Sci.* 1: 517–529.

Marshall, S. K., Spainhower, K. B., Sinn, B. T., Diggins, T. P. and Butcher, M. T. (2021) Hind limb bone proportions reveal unexpected morphofunctional diversification in xenarthrans. *J. Mammal. Evol.* 1–21.10.1007/s10914-021-09537-w

Medler, S. (2002) Comparative trends in shortening velocity and force production in skeletal muscles. *Am. J. Physiol.* 283: R368–R378.

Mendel, F. C. (1981a). Use of hands and feet of two-toed sloths (*Choloepus hoffmanni*) during climbing and terrestrial locomotion. *J. Mammal*. 62: 413–421.

Mendel, F. C. (1981b). The hand of two-toed sloths (Choloepus): Its anatomy and potential uses relative to size of support. *J. Morphol*. 169: 1–19.

Mendel, F. C. (1985a). Use of hands and feet of three-toed sloths (*Bradypus variegatus*) during climbing and terrestrial locomotion. *J. Mammal*. 66: 359–366.

Mendel, F. C. (1985b). Adaptations for suspensory behavior in the limbs of two-toed sloths. In The Ecology and Evolution of Armadillos, Sloths, and Vermilinguas. Smithsonian Institute Press (ed. G. G. Montgomery), pp. 151–162. Washington, DC: Smithsonian Institution Press.

Mendez, J. and Keyes, A. (1960). Density and composition of mammalian muscle. *Metabolism* 9: 184–188.

Meritt, D. A., Jr. (1985). The two-toed Hoffmann's sloth, Choloepus hoffmanni. In The evolution and ecology of armadillos, sloths, and vermilinguas (ed. G. G. Montgomery) pp. 333–341. Washington, DC: Smithsonian Institution Press.

Montgomery, G. G. and Sunquist, M. E. (1975). Impact of sloths on neotropical forest energy flow and nutrient cycling. In Tropical ecological systems: Trends in terrestrial and aquatic research (eds. F. B. Golley and E. Medina), pp. 69–98. New York: Springer Verlag.

Montgomery, G. G. and Sunquist, M. E. (1978). Habitat selection and use by two-toed and three-toed sloths. In The ecology of arboreal folivores (ed. G. G. Montgomery), pp. 329–359. Washington, DC: Smithsonian Institution Press.

Montgomery, G. G. (1983). Bradypus variegatus (perezoso de tres dedos, three-toed sloth). In Costa Rican natural history (ed. D. H. Janzen), pp. 453–456. Chicago: University of Chicago Press.

Moore, A. L., Budny, J. E., Russell, A. P. and Butcher, M. T. (2013). Architectural specialization of the intrinsic forelimb musculature of the American badger (*Taxidea taxus*). *J. Morphol*. 274: 35–48.

Mossor, A. M., Austin, B. L., Avey-Arroyo, J. A. and Butcher, M.T. (2020) Horses hanging upside down?: Tensile strength and elasticity of sloth flexor tendons. *Integr. Org. Biol.* 2: 1–11. https://doi.org/10.1093/iob/obaa032

Muchlinski, M. N., Snodgrass, J. J. and Terranova, C. J. (2012). Muscle mass scaling in primates: An energetic and ecological perspective. *Am. J. Primatol*. 74: 395–407.

Muscolino, J. E. (2011). Kinesiology: The skeletal system and muscle function, 15th ed. Chicago, Illinois: Mosby/Elsevier: 704.

Muybridge, E. (1887). The Horse in motion. "Sallie Gardner," owned by Leland Stanford; running at a 1:40 gait over the Palo Alto track. California Palo Alto, ca.

Nyakatura, J. A. and Fischer, M. S. (2010). Three-dimensional kinematic analysis of the pectoral girdle during upside-down locomotion of two-toed sloths (*Choloepus didactylus*, Linné 1758). *Front. Zool*. 7: 21.

Nyakatura, J. A., Petrovitch, A. and Fischer, M. S. (2010). Limb kinematics during locomotion in the two-toed sloth (*Choloepus didactylus*, Xenarthra) and its implications for the evolution of the sloth locomotor apparatus. *Zool*. 113: 221–234.

Nyakatura, J. A. (2012). The convergent evolution of suspensory posture and locomotion in tree sloths. *J. Mamm. Evol*. 19: 225–234.

Nyakatura, J. A. and Andrada, E. (2013). A mechanical link model of two-toed sloths: No pendular mechanics during suspensory locomotion. *Acta Theriol*. 58: 83–93.

Olson, R. A., Glenn, Z. G., Cliffe, R. N. and Butcher, M. T. (2018). Architectural properties of sloth forelimb muscles (Pilosa: Bradypodidae). *J. Mamm. Evol*. 25: 573–588.

Pate, E., Wilson, G. J., Bhimani, M. and Cooke, R. (1994). Temperature dependence of the inhibitory effects of orthovanadate on shortening velocity in fast skeletal muscle. *Biophys J* 66: 1554–1562.

Pauli, J. N., Peery, M. Z., Fountain, E. D. and Karasov, W. H. (2016). Arboreal folivores limit their energetic output, all the way to slothfulness. *Am. Nat*. 188: 196–204.

Payne, R. C., Hutchinson, J. R., Robilliard, J. J., Smith, N. C. and Wilson, A. M. (2005). Functional specialisation of pelvic limb anatomy in horses (*Equus caballus*). *J. Anat.* 206: 557–574.

Presslee, S., Slater, G., Pujos, F., Forasiepi, A., Fischer, R., Molloy, K. Mackie, M., Olsen, J., Kramarz, A., Taglioretti, M., Scaglia, F., Lezcano, M., Lanata, J., Southon, J., Feranec, R., Bloch, J., Hajduk, A., Martin, F., Salas-Gismondi, R. and Macphee, R. (2019). Palaeoproteomics resolves sloth relationships. *Nature Ecol. Evol*. 3: 1–10.

Pujos, F., Gaudin, T. J., De Iuliis, G. and Cartelle, C. (2012). Recent advances on variability, morpho-functional adaptations, dental terminology, and evolution of sloths. *J. Mamm. Evol*. 19, 159–169.

Ranatunga, K. W. (1996). Endothermic force generation in fast and slow mammalian (rabbit) muscle fibers. *Biophys. J*. 71: 1905–1913.

Rose, J. A., Sandefur, A., Huskey, S., Demler, J. L. and Butcher, M. T. (2013). Muscle architecture and out-force potential of the thoracic limb in the eastern mole (*Scalopus aquaticus*). *J. Morphol*. 274: 1277–1287.

Rupert, J. E., Rose, J. A., Organ J. M. and Butcher, M. T. (2015). Forelimb muscle architecture and myosin isoform composition in the groundhog (*Marmota monax*). *J. Exp. Biol*. 218: 194–205.

Schiaffino, S. and Reggiani, C. (1996). Molecular diversity of myofibrillar proteins: gene regulation and functional significance. *Physiol. Rev*. 76: 371–423.

Schmidt, M. (2008). Forelimb proportions and kinematics: How are small primates different from other small mammals? *J. Exp. Biol*. 211: 3775–3789.

Schmitt, D. and Lemelin, P. (2004). Locomotor mechanics of the slender loris (*Loris tardigradus*). *J. Hum. Evol*. 47: 85–94.

Sickles, D.W. and Pinkstaff, C.A. (1981). Comparative histochemical study of prosimian primate hindlimb muscles. I. Muscle fiber types. *Am. J. Anat*. 160: 175–186.

Sickles, D.W. and Pinkstaff, C.A. (1981). Comparative histochemical study of prosimian primate hindlimb muscles. II. Populations of fiber types. *Am. J. Anat*. 160: 187–194.

Spainhower, K. B., Cliffe, R. N., Metz, A. K., Barkett, E. M., Kiraly, P. M., Thomas, D. R., Kennedy, S. J., Avey-Arroyo, J. A. and Butcher, M. T. (2018a). Cheap Labor: Myosin fiber type expression and enzyme activity in the forelimb musculature of sloths (Pilosa: Xenarthra). *J. Appl. Physiol*. 125: 799–811.

Spainhower, K., Metz, A. K., Kiraly, P. M., Thomas, D. R. and Butcher, M. T. (2017). Fiber type properties of the limb muscles of sloths (Xenarthra: Pilosa). *Integr. Comp. Biol.* 57(suppl 1): e414, 227.

Spainhower, K. B., Metz, A. K., Yusuf, A-R. S., Johnson, L. E., Avey-Arroyo, J. A. and Butcher M. T. (2021). Coming to grips with life upside down: how myosin fiber type and metabolic characteristics of sloth hindlimbs contribute to suspensory function. *J. Comp. Physiol. B* 191: 207-224. doi: 10.1007/s00360-020-01325-x

Sunquist, M. E. and Montgomery, G. G. (1973). Activity patterns and rates of movement of two-toed and three-toed sloths (*Choloepus hoffmanni* and *Bradypus infuscatus*). *J. Mammal*. 54: 946–954.

Thomas, D. R., Chadwell, B. A., Walker, G. R., Budde, J. E., VandeBerg, J. L. and Butcher, M.T. (2017). Ontogeny of myosin isoform expression and prehensile function in the tail of the gray short-tailed opossum *(Monodelphis domestica). J. Appl. Physiol.* 123: 513–525.

Toniolo, L., Maccatrozzo, L., Patruno, M., Pavan, E., Caliaro, F., Rossi, R., Rinaldi, C., Canepari, M., Reggiani, C. and Mascarello, F. (2007). Fiber types in canine muscles: myosin isoform expression and functional characterization. *Am. J. Physiol.* 292: C1915–C1926.

Touchton, J. M., Hsu, Y. C. and Palleroni, A. (2002). Foraging ecology of reintroduced captive-bred subadult harpy eagles (*Harpia harpyja*) on Barro Colorado Island, Panama. *Ornithol. Neotrop*. 13: 365–379.

Urbani, B. and Bosque, C. (2007). Feeding ecology and postural behaviour of the three-toed sloth (*Bradypus variegatus*) in northern Venezuela. *Mammal. Biol.* 72: 321–329.

Usherwood, J.R. and Davies, Z. T. (2017). Work minimization accounts for footfall phasing in slow quadrupedal gaits. *eLife* 6: e29495. doi 10.7554/eLife.29495

Vaughn, C., Ramírez, O., Herrera, G. and Guries, R. (2007). Spatial ecology and conservation of two sloth species in a cacao landscape in Limón, Costa Rica. *Biodivers. Conserv*. 16: 2293–2310.

Vizcaíno, S. F., Bargo, M. S. and Fariña, R. A. (2008). Form, function, and paleobiology in xenarthrans. In: The biology of the xenarthra (eds. S. F. Vizcaíno and W. J. Loughry), pp. 86-99. Gainesville: University Press of Florida.

Vizcaíno, S. F. (2009). The teeth of the "toothless": Novelties and key innovations in the evolution of xenarthrans (Mammalia, Xenarthra). *Paleobiology* 35: 343–366.

Voirin, B., Scriba, M. F., Martinez-Gonzalez, D., Vyssotski, A. L., Wikelski, M. and Rattenborg, N. C. (2014). Ecology and Neurophysiology of Sleep in Two Wild Sloth Species. *Sleep*. 37: 753–761.

Williams, S. B., Payne, R. C. and Wilson, A. M. (2007a) Functional specialisation of the pelvic limb of the hare (*Lepus europeus*). *J. Anat.* 210: 472–490.

Williams, S. B., Payne, R. C. and Wilson, A. M. (2007b) Functional specialisation of the thoracic limb of the hare (*Lepus europeus*). *J. Anat.* 210: 491–505.

Williams, S. B., Wilson, A. M., Daynes, J., Peckham, K. and Payne, R. C. (2008a) Functional anatomy and muscle moment arms of the thoracic limb of an elite sprinting athlete: the racing greyhound (*Canis familiaris*). *J. Anat.* 213: 373–382.

Williams, S. B., Wilson, A. M., Rhodes, L., Andrews, J. and Payne, R. C. (2008b). Functional anatomy and muscle moment arms of the pelvic limb of an elite sprinting athlete: the racing greyhound (*Canis familiaris*). *J Anat.* 213: 361–372.

Windle, B. C. A. and Parsons, F. G. (1899). On the myology of the Edentata. *Proc. Zool. Soc., Lond*. 990–1017.

Wislocki, G. B. (1928). Observations on the gross and microscopic anatomy of the sloths (*Bradypus griseus griseus* Gray and *Choloepus hoffmanni* Peters). *J. Morphol*. 46: 317–397.

Woledge, R. C., Curtin, N. A. and Homsher, E. (1985). Energetic aspects of muscle contraction. *Monograph Physiol. Soc.* 41: 1–357.

Zajac F. E. (1989). Muscle and tendon: properties, models, scaling, and application to biomechanics and motor control. *Crit. Rev. Biomed. Eng.* 17: 359–411.

Zajac, F. E. (1992). Muscle coordination of movement: a perspective. *J. Biomech.* 26: 109–124.

Table 1 Origins, insertions, and fiber architecture for all hindlimb muscles of *B. variegatus*.

Muscle	Abbrev.	Origin	Insertion	Fiber Architecture
Hip region				
Iliopsoas	ILPS	Iliac fossa; transverse processes L1-L4; ventrolateral sacrum	Lesser trochanter of femur	parallel/ unipennate
Psoas minor	PMN	Body of terminal thoracic vertebrae	Iliopectineal margin of illium	parallel
Tensor fascia latae	TFL	Tuber coxae of ilium	Fascia latae on lateral femur	parallel
Gluteus superficialis	GLS	Iliac crest, lateral margin of sacrum	Femur distal to greater trochanter; fascia latae	parallel
Gluteus medius	GLM	Dorsal body of ilium	Greater trochanter of femur	parallel
Gluteus profundus	GLP	Caudal aspect of dorsal ilium	Greater trochanter of femur	parallel
Piriformis	PFM	Ventral border of sacrum	Caudal aspect of greater trochanter	parallel
Gemelli	GEM	Lateral surface of ischial tuberosity	Base of greater trochanter	parallel
Quadratus femoris	QF	Lateral body of ischium	Distal, caudal aspect of greater trochanter	parallel
Obturator externus	OE	Caudolateral body of pubis, pubic ramus, obturator membrane	Caudal aspect of greater trochanter	parallel
Obturator internus	OI	Obturator membrane, cranioventral body of pubis	Trochanteric fossa; joint capsule of hip	parallel
Thigh region				
Sartorius	SRT	Cranial aspect of tuber coxae	Distal, medial femur; medial condyle of tibia	parallel/ unipennate
Gracilis	GRC	Iliopubic ramus, body of pubis, pubic symphysis	Medial condyle of tibia and shaft; thick crural fascia of caudal leg	parallel
Pectineus	PCT	Pectineal ridge of ilium	Medial femoral mid-shaft	parallel/ bipennate
Adductor				
– brevis	ADDB	Cranial 1/4 iliopubic ramus	Proximal 2/3 caudomedial femur	parallel

– longus [a]	ADDL	Iliopubic ramus	Distal 1/3 caudomedial femur, medial femoral epicondyle	parallel
– magnus	ADDM	Caudal 1/4 iliopubic ramus, pubic tubercle	Middle 1/3 caudal femur	parallel
Semitendinosus	ST	Dorsal ischiopubic ramus, ischial tuberosity	Caudal aspect of medial condyle of tibia; medial femoral epicondyle [b]	parallel
Semimembranosus	SM	Ischial tuberosity, ischiopubic ramus	Medial condyle of tibia; caudomedial, distal femur; crural fascia	parallel
Biceps femoris – long	BFL	Dorsocaudal ischial tuberosity, ischiopubic ramus	Proximal 1/4 fibula; superficial layer of crural fascia	parallel
Biceps femoris – short	BFS	Distal greater trochanter, proximal 1/2 caudolateral femoral shaft	Fibular mid-shaft; deep layer of crural fascia	parallel
Quadriceps femoris				
Rectus femoris	RF	Ilium, cranioventral lip of acetabulum		parallel
Vastus intermedius [c]	VI	Femoral head, entire length of cranial femoral shaft	Patella; tibial tuberosity via patellar ligament	parallel
Vastus lateralis	VL	Femoral head, craniolateral surface of greater trochanter and femoral shaft		unipennate
Vastus medialis	VM	Base of the femoral neck, craniomedial femoral shaft		unipennate
Leg region				
Gastrocnemius – medial	MG	Caudal aspect of medial condyle of femur	Dorsal projection of calcaneus	parallel
Gastrocnemius – lateral	LG	Caudolateral aspect of distal femur	Dorsal projection of calcaneus	parallel/ unipennate
Soleus	SOL	Proximal 2/3 caudal fibula	Dorsomedial surface of calcaneus	parallel/ unipennate
Popliteus	POP	Caudal aspect of lateral femoral epicondyle (contains sesamoid bone)	Caudal aspect of medial tibial condyle	unipennate
Flexor digitorum superficialis	FDS	Caudolateral aspect of distal femoral shaft, lateral epicondyle of femur	Common flexor tendon of FDP	unipennate/bipennate
Flexores digitorum profundi	FDP	Caudomedial tibial shaft; interosseous membrane; caudal fibular head and shaft	Distal phalanx of digits II-IV (via three flexor tendons and volar tunnels)	unipennate
Tibialis caudalis	TCD	Caudal surfaces of tibial shaft and inner medial condyle	Base of remnant metatarsal I	parallel

Fibularis longus	FL	Craniolateral femoral condyle; fibular head and proximal 1/2 shaft	Tuberosity of remnant metatarsal V, base of metatarsal IV	parallel
Fibularis brevis	FB	Distal 1/2 lateral fibular shaft and lateral malleolus of fibula	Base of tuberosity of metatarsal V	parallel
Fuibularis tertius [d]	FT	Cranial aspect of lateral tibial condyle	Doral aspect of base of metatarsal IV	
Fibularis quartus	FQ	Distolateral fibula	Lateral aspect of calcaneus	parallel
Extensor digitorum lateralis [e]	EDLA	Caudolateral fibular shaft	Metatarsal IV, lateral aspect of tuberosity of metatarsal V	parallel
Extensor digitorum longus	EDLO	Cranial aspect of lateral tibial condyle; Fibular head; lateral femoral condyle	Dorsal aspect of base of metatarsal III	parallel
Tibialis cranialis – tibial	TCN-t	Medial condyle of tibia and tibial tuberosity; Fibular head	Lateral aspect of remnant metatarsal I	parallel
Tibialis cranialis – fibular et tibial	TCN-ft	Distal 1/2 craniomedial fibula	Lateral aspect of remnant metatarsal I (via common tendon)	parallel
Tibialis cranialis – fibular	TCN-f	Distal, cranial fibula and lateral malleolus; distolateral tibia	Dorsomedial aspect of base of remnant metatarsal I	parallel
Foot region				
Quadratus plantae	QP	Medial, plantar, and lateral surfaces of calcaneus	Flexor tendons of digits (3; proximal to volar tunnels)	parallel
Flexor digitorum brevis [f]	FDB	Calcaneus (via tendon/muscle slips)	Distal, lateral aspect of metatarsal IV	parallel
Extensor digitorum brevis	EDB	Dorsal surface of tarsals; proximal end of metatarsals II-IV	Distal end of intermediate phalanx, base of distal phalanx of digits II-IV	parallel
Interossei	IOS	Medial/lateral aspects of metatarsals I-V; tarsal bones	Proximal/intermediate phalanges of digits II-IV; tendon expansions of EDB	bipennate
Lumbricales [g]	LUM	Plantar aspect of foot (as tendon/muscle slips of unclear origin)	Lateral aspect of remnant metatarsal V	parallel

a, m. adductor longus has cranial and caudal heads; b, observed in two individuals; c, additionally originated from acetabulum in three individuals from which a muscle moment arm was measured; d-e, possibly a sub-division of fibers from m. fibularus longus; f-g, not clearly observed/present in all individuals.

Table 2 Muscle functional groups used for analysis.

Muscles studied and Muscle groups
Hip flexors Iliopsoas, Psoas minor[a], Sartorius, Rectus femoris, Tensor fascia latae, Gluteus superficialis, Vastus intermedius[b]
Hip extensors Gluteus medius (Fused with: Piriformis and Gluteus profundus), Biceps femoris (long head), Semimembranosus, Semitendinosus
Femoral Rotators/Stabilizers Quadratus femoris, Obturator internus, Obturator externus, Gemelli (inferior, superior)
Hip abductors Gluteus superficialis, Gluteus medius, Gluteus profundus[c]
Hip adductors Gracilis, Adductor magnus, Adductor longus (heads: cranial, caudal), Adductor brevis, Pectineus
Knee flexors Sartorius, Biceps femoris (short head), Biceps femoris (long head), Semimembranosus, Semitendinosus, Gracilis, Popliteus, Gastrocnemius (heads: medial, lateral), Flexor digitorum superficialis (i.e., Plantaris)
Knee extensors Vastus lateralis, Vastus medialis, Vastus intermedius, Rectus femoris
Ankle flexors Tibialis cranialis (tibial head), Tibialis cranialis (tibial et fibular head), Tibialis cranialis (fibular head), Fibularis longus (i.e., Peroneus longus), Extensor digitorum longus[d]
Ankle extensors Gastrocnemius (heads: medial, lateral), Soleus, Tibialis caudalis, Fibularis quartus (i.e., Peroneus quartus)
Digital flexors Flexor digitorum superficialis, Flexores digitorum profundi, Quadratus plantae,
Digital extensors Extensor digitorum brevis
Ankle/Foot Supinators Tibialis cranialis (3 muscle complex)[e], Tibialis caudalis
Ankle/Foot/Leg Pronators Popliteus, Fibularis quartus, Fibularis longus, Fibularis brevis (i.e., Peroneus brevis)
Digital Abductors Interossei (medial, central, lateral)[f]

a, portion of the muscle belly is fused with m. psoas major can assist hip flexion; b, additionally originated from acetabulum in three individuals with a short, flexor muscle arm; c, muscle was clearly separable in one individual; d, inserts onto bas of metatarsal III and can only act to flex the foot at the ankle joint; e, fused muscle complex comprising modified flexor/supinator muscles from the former m. extensor digit I longus and brevis; f, analyzed only for mass.

Table 3 Architectural measurements (raw data) for all hindlimb muscles of *B. variegatus*.

Muscle	Age	Muscle mass (g)	Muscle length (cm)	Fascicle length (cm)	Pennation angle (°)	PCSA (cm^2)	Fmax (N)
ILPS	A	10.9±3.9	10.3±2.0	5.03±1.1	19	2.24±1.0	67.3±30
	J	3.0±0.0	5.04±2.5	3.50±0.9	0	0.79±0.1	23.9±2.9
PMN	A	3.63±1.4	8.35±2.7	3.28±0.8	0	1.03±0.3	31.0±9.4
	J	0.8	4.08	1.68±0.5	0	0.45	13.5
TFL	A	1.74±0.8	5.60±0.9	4.99±1.1	0	0.34±0.1	10.1±3.4
	J	0.25±0.1	3.52±0.3	2.59±0.5	0	0.11	3.28
GLS	A	7.08±2.9	8.57±1.5	5.04±1.3	0	1.33±0.5	40.0±15
	J	1.20±0.3	4.30±1.4	3.96±0.6	0	0.33	10.0
GLM	A	10.0±4.0	6.09±0.7	4.47±1.2	0	2.06±0.6	61.8±5.3
	J	2.30±0.7	5.13±2.8	2.68±0.6	0	0.99	29.6
GLP	A	8.82±0.02	4.14	2.99±1.3	0	0.44	13.3
	J	--	--	--	--	--	--
PFM	A	3.33±0.8	6.52±2.1	3.91±0.9	0	0.64±0.0	19.1±1.5
	J	0.60	3.90	3.90±0.7	0	0.15	4.35
GEM	A	1.45±0.6	2.44±0.1	1.80±0.2	0	1.03	31.0
	J	0.35	2.10	1.64±0.2	0	0.20	6.05
QF	A	2.68±1.6	5.14±0.7	3.49±0.9	0	0.74±0.5	22.2±15
	J	0.75±0.4	3.75±0.6	2.62±0.4	0	0.18	5.25
OE	A	5.17±2.5	4.72±0.3	3.63±0.7	0	1.38±0.7	41.3±22
	J	1.0	3.41	--	--	--	--
OI	A	0.46±0.1	2.57±0.3	2.30±0.4	0	0.21±0.1	6.17±1.6
	J	0.20±0.0	2.04±0.3	--	--	--	--
SRT	A	3.36±1.4	9.33±1.0	6.83±1.5	13	0.56±0.2	16.9±6.3
	J	0.45±0.2	5.46±1.0	4.73±0.8	0	0.10±0.1	3.02±2.0
GRC	A	8.24±3.7	11.3±2.6	8.49±2.1	0	0.92±0.4	27.5±11
	J	1.40±1.0	8.00±1.8	6.52±1.2	0	0.18±0.1	5.52±3.2
PCT	A	4.00±0.8	6.93±1.0	3.36±0.8	0	1.27±0.1	38.1±3.8
	J	1.00±0.4	4.40	1.53±0.4	8	0.43	12.8
ADDB	A	3.09±0.6	6.10±0.5	3.62±1.1	0	0.88±0.2	26.5±6.7
	J	0.62	4.19	2.93±0.5	0	0.20	5.97
ADDL	A	3.44±1.2	8.24±1.1	6.09±1.2	0	0.54±0.2	16.1±5.5
	J	0.69±0.0	5.12±1.7	4.28±1.4	0	0.15	4.52
ADDM	A	3.00±1.0	7.92±0.8	6.12±0.9	0	0.47±0.2	14.1±4.8
	J	0.90±0.3	5.53±0.5	4.65±0.7	0	0.22	6.70
ST	A	3.94±1.4	9.59±1.1	6.83±1.5	0	0.56±0.2	16.8±6.7
	J	0.55±0.2	5.72±0.5	4.03±0.9	0	0.13±0.0	3.79±0.6
SM	A	9.48±3.9	10.6±2.3	8.76±1.5	0	1.05±0.3	31.6±10
	J	2.35±1.1	7.19±2.0	5.64±1.4	0	0.36±0.1	10.7±1.7
BFL	A	2.92±1.8	9.34±3.0	7.31±2.7	0	0.36±0.1	10.9±4.3

	J	0.60±0.4	6.38±1.7	5.10±0.7	0	0.10±0.1	3.11±1.8
BFS	A	4.42±2.1	12.0±1.1	7.35±2.6	0	0.55±0.2	16.6±5.3
	J	1.05±0.5	7.30±2.7	5.89±1.9	0	0.16±0.0	4.82±0.9
RF	A	3.00±2.1	7.60±1.4	4.07±1.8	16±8	0.70±0.5	20.9±15
	J	0.72±0.7	5.62	3.29±0.9	0	0.34	10.3
VI	A	2.69±1.5	7.79±2.0	3.77±2.7	15	0.82±0.2	24.5±7.0
	J	0.34±0.0	4.50	1.88±0.7	12±5	0.13	4.01
VL	A	2.23±0.6	7.48±0.8	2.43±0.9	22±8	0.88±0.2	26.3±6.9
	J	0.43±0.2	4.83±1.0	1.37±0.3	16±4	0.28±0.1	8.41±3.4
VM	A	3.22±1.0	7.94±1.3	3.12±1.9	18±7	1.14±0.6	34.3±19
	J	0.81±0.0	4.95±0.07	2.13±0.9	12±5	0.42±0.2	12.6±7.1
MG	A	2.80±1.4	10.0±2.1	7.89±1.7	0	0.32±0.1	8.58±3.7
	J	0.60±0.3	6.46±2.5	5.42±1.5	0	0.10±0.0	3.04±0.6
LG	A	2.54±1.2	11.6±1.6	8.07±2.3	7	0.29±0.1	9.66±4.2
	J	0.75±0.1	7.47±0.40	6.28±0.8	0	0.11±0.0	3.41±0.7
SOL	A	2.62±1.1	8.66±0.84	5.94±1.5	12	0.42±0.2	12.6±5.9
	J	0.50	6.42	4.31±0.4	0	0.11	3.28
POP	A	2.05±0.5	4.39±0.7	2.42±0.6	15±7	0.76±0.2	22.7±5.3
	J	0.35±0.2	2.61±0.3	1.50±0.4	23	0.21±0.1	6.26±3.5
FDS	A	10.4±4.1	8.02±1.2	5.95±1.9	0	1.64±0.6	49.1±18
	J	2.20±0.7	4.50	4.16±1.3	18	0.45±0.0	13.6±1.5
FDP	A	12.2±3.9	7.03±1.7	3.89±1.5	20±11	3.13±0.9	93.8±26
	J	3.85±2.3	5.95±1.1	1.69±0.8	15	1.81±0.3	54.3±9.0
TCD	A	1.88±1.0	7.23±1.4	3.52±1.3	8±3	0.41±0.1	12.4±4.5
	J	0.20±0.0	5.34±1.3	1.74±0.4	0	0.11	3.25
FL	A	4.30±2.1	10.4±0.7	5.53±2.0	11	0.69±0.3	20.8±8.8
	J	0.70±0.4	5.10	3.52±0.7	0	0.11	3.22
FB	A	1.38±0.5	5.23±1.6	3.18±1.3	0	0.37±0.1	11.0±2.8
	J	0.45±0.2	2.11	1.31±0.3	0	0.43	12.9
*EDLA	A	1.40	9.23	2.66±1.0	6	0.49	14.8
	J	1.00	6.69	4.69±0.9	0	0.20	6.03
FQ	A	0.983±0.4	3.42	2.65±0.6	6	0.32	9.63
	J	0.10	2.20	1.98±0.1	0	0.05	1.43
EDLO	A	5.40±3.1	10.4±0.5	7.36±1.5	9	0.66±0.3	19.7±9.4
	J	1.00±0.6	6.46±1.4	4.89±1.2	0	0.17±0.0	5.15±1.5
TCN-t	A	3.59±1.6	9.31±1.0	5.69±1.7	24	0.50±0.2	14.9±6.2
	J	0.71±0.3	3.70	2.66±0.9	0	0.24±0.0	7.18±1.5
TCN-ft	A	5.20±1.7	7.28±1.3	4.81±1.8	0	1.30±0.4	39.1±13
	J	0.97±0.4			0		
TCN-f	A	2.06±1.0	3.23±0.5	2.27±0.5	0	0.84±0.3	25.3±10.5
	J	0.42±0.0	2.00	1.80±0.3	0	0.21	6.29

QP	A	5.12±1.2	4.25±0.4	3.20±0.6	0	1.53±0.3	46.0±8.1
	J	1.45±0.6	2.76±0.5	2.26±0.4	0	0.59±0.1	17.7±4.4
*FDB	A	2.00±0.5	3.42±1.4	2.162±0.2	0	0.19	5.59
	J	0.10	1.60				
EDB	A	1.77±0.5	4.60±1.5	3.17±0.8	0	0.57±0.2	17.1±5.0
	J	0.70±0.6	4.62	--	--	--	--
IOS	A	2.15±0.8	--	--	--	--	--
	J	0.10	--	--	--	--	--
LUM	A	0.80±0.4	3.43±1.5				
	J	--	--	--	--	--	--

Values are mean ± s.d. (standard deviation)
A, adult; J, juvenile

Table 4 Muscle moment arms (r_m) and functional data (joint torque, power) for selected hindlimb muscles of *B. variegatus*.

Joint	Muscle	Age	Mean r_m (cm)	Joint Torque (N.cm kg^{-1})	Summed Torque	Power (W kg^{-1})
Hip	ILPS	A	1.63±0.5	34.7±23.8		0.19±0.06
		J	2.00±1.4			
	PMN	A	--	--		0.06±0.02
		J	--			
	TFL	A	1.84±0.2	4.64±1.6		0.03±0.01
		J	1.03			
	GLS	A	1.01±0.7	8.89±4.5		0.12±0.05
		J	0.58±0.1			
	SRT	A	3.80±0.5	13.23±9.1		0.05±0.03
		J	1.84±0.3			
	*VI	A	1.07±0.3	7.07		0.04±0.02
		J	1.02			
	RF	A	1.17±0.4	7.02±4.4	**Flexors 75.0**	0.06±0.04
		J	0.78			
	GLM	A	0.70±0.2	10.90±3.1		0.16±0.04
		J	0.33			
	GLP	A	0.69	2.29		0.02
		J	--			
	PFM	A	0.79±0.3	4.82		0.04±0.003
		J	--			
	BFL	A	1.84±0.6	6.18±3.7		0.05±0.03
		J	1.28			
	SM	A	2.4±0.6	19.79±6.7		0.16±0.07
		J	1.81			
	ST	A	1.64±0.2	6.98±3.3	**Extensors 51.0**	0.06±0.03
		J	1.28			
Knee	SRT	A	1.48	8.22		0.05±0.03
		J	--			
	GRC	A	2.39±0.8	17.1±10.0		0.12±0.06
		J	2.05			
	SM	A	2.18±0.4	17.9±4.7		0.16±0.07
		J	1.36			
	ST	A	1.09±0.4	4.85±1.6		0.06±0.03
		J	--			
	BFL	A	2.26±0.7	6.24±4.2		0.05±0.03
		J	0.90			
	BFS	A	3.56±1.1	15.6±8.4		0.07±0.03
		J	2.05			
	MG	A	1.06±0.3	2.73±1.5		0.04±0.02
		J	0.61			

	LG	A J	2.38±1.0 1.38	5.27±3.3		0.05±0.02
	POP	A J	0.85±0.1 --	5.03±1.0		0.03±0.01
	FDS	A J	1.34±0.3 0.63	15.5±8.6	**Flexors 98.3**	0.16±0.06
	RF	A J	1.00±0.3 1.07	7.08±5.5		0.06±0.04
	VI	A J	1.50 --	6.50		0.04±0.02
	VL	A J	0.83±0.3 1.07	6.99±2.7		0.03±0.01
	VM	A J	1.23±0.4 0.95	13.4±5.0	**Extensors 34.0**	0.05±0.01
Ankle	FL	A J	1.14±0.3 0.77	6.25±3.0		0.07±0.04
	EDLO	A J	1.71±0.5 1.26	9.23±4.1		0.08±0.04
	TCN-t	A J	0.79±0.1 --	3.50±1.7		0.05±0.03
	TCN-ft	A J	0.73±0.1 --	8.42±3.5		0.10±0.02
	TCN-f	A J	0.79±0.1 --	5.46±2.5	**Flexors 33.0**	0.03±0.01
	MG	A J	1.79±0.6 1.02	4.26±1.9		0.04±0.02
	LG	A J	2.00±0.3 1.02	4.10±1.3		0.05±0.02
	SOL	A J	1.6±0.3 1.43	5.10±2.4		0.04±0.02
	TCD	A J	0.67±0.1 0.56	2.64±1.4		0.02±0.01
	FQ	A J	0.59±0.3 --	2.17	**Extensors 18.3**	0.01±0.01
Digits	FDS	A J	1.14±0.4 0.45	12.72±8.2		0.16±0.06
	FDP	A J	1.13±0.1 0.43	33.5±11.0		0.21±0.08
	QP	A J J	1.23±0.1 -- --	16.54±3.7	**Flexors 62.8**	0.09±0.02

All values are mean ± s.d. (standard deviation)
r_m is moment arm length

Fig. 1 Distribution of muscle functional group physiological cross-sectional area (PCSA) to total hindlimb PCSA in *B. variegatus*. Total hindlimb PCSA was calculated as the summed PCSA of all hindlimb muscles studied (n=46) from N=7 individuals. Proximal-to-distal muscle group PCSA is expressed as a percentage, with *bars* representing means for each functional group and *error bars* the s.d. (standard deviation). Muscles with synergistic primary actions are combined in a functional group. Muscles with secondary actions are included in more than one functional group as are bi-articular muscles.

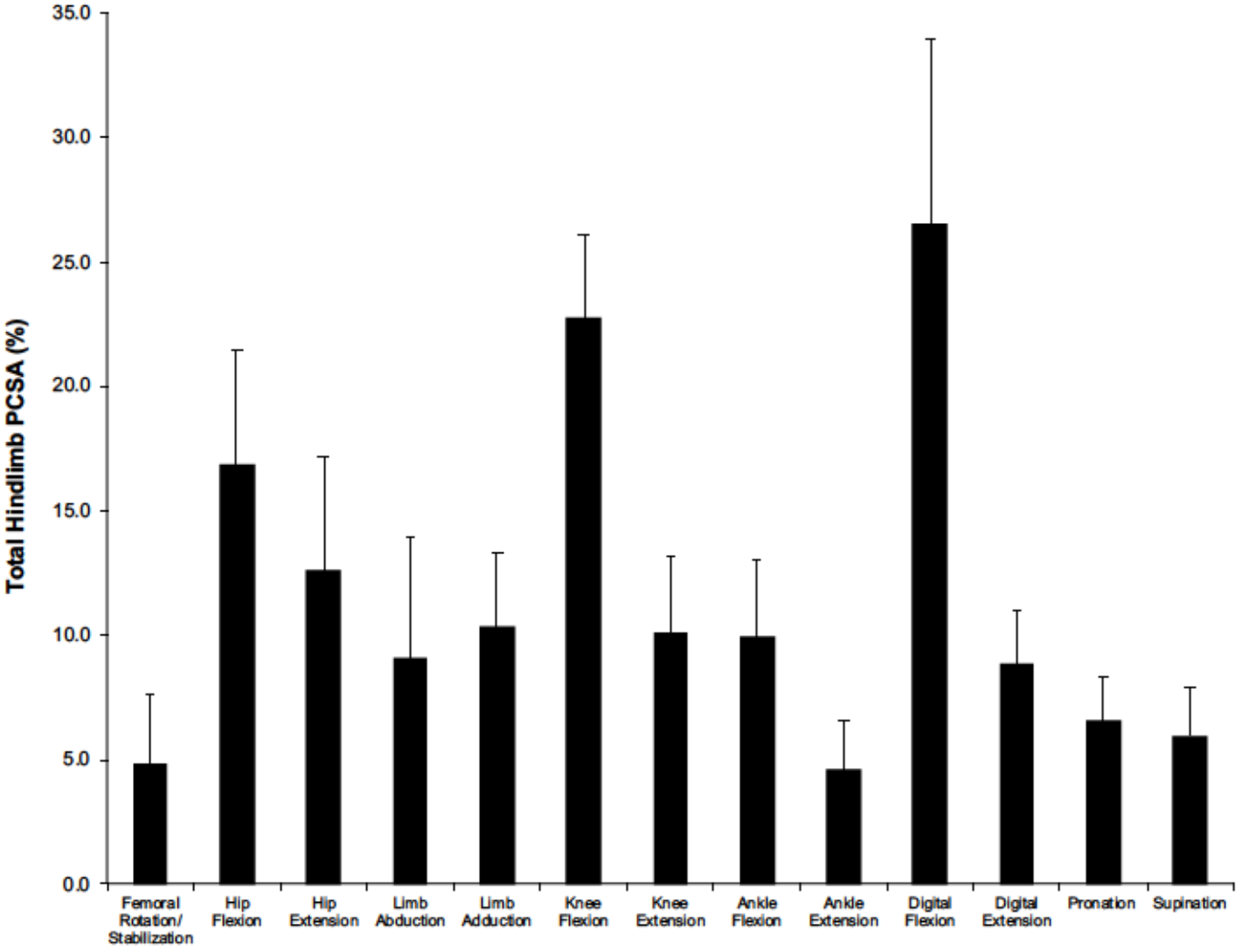
Total Hindlimb PCSA (%)
35.0
30.0
25.0
20.0
15.0
10.0
5.0
0.0
Femoral Rotation/ Stabilization
Hip Flexion
Hip Extension
Limb Abduction
Limb Adduction
Knee Flexion
Knee Extension
Ankle Flexion
Ankle Extension
Digital Flexion
Digital Extension
Pronation
Supination

Fig. 2 Functional space plots for muscles with large relative power, joint torque, and joint rotational velocity in the hindlimb of *B. variegatus*. **A.** Normalized PCSA as a function of normalized fascicle length (L_F). PCSA is normalized to body mass $(BM)^{0.67}$ and fascicle length to $(BM)^{0.33}$. **B.** Normalized PCSA as a function of normalized muscle moment arm (r_m). Measurements for r_m are normalized to body mass $(BM)^{0.33}$. **C.** Normalized L_F as a function of normalized r_m. Data *points* are means shown with no *error bars*. Selected muscles are labeled in each panel. Muscles that produce large force (large PCSA) and are capable of large excursion and shortening velocity (long L_F) have the capacity for high power output (upper right quadrant in **A**); both large PCSA and long r_m are muscles capable of applying large joint torque (upper right quadrant in **B**); both long L_F and short r_m are muscles capable of fast joint rotational velocity (upper left quadrant in **C**). The 'torque range modified' area is defined as muscles with relatively long L_F, and r_m. Generalized muscles have relatively small PCSA and both short fascicle and moment arm lengths. Red data points are muscle capable of high power; blue points large force; green points excursion/velocity. Muscle abbreviations are defined in Table 1.

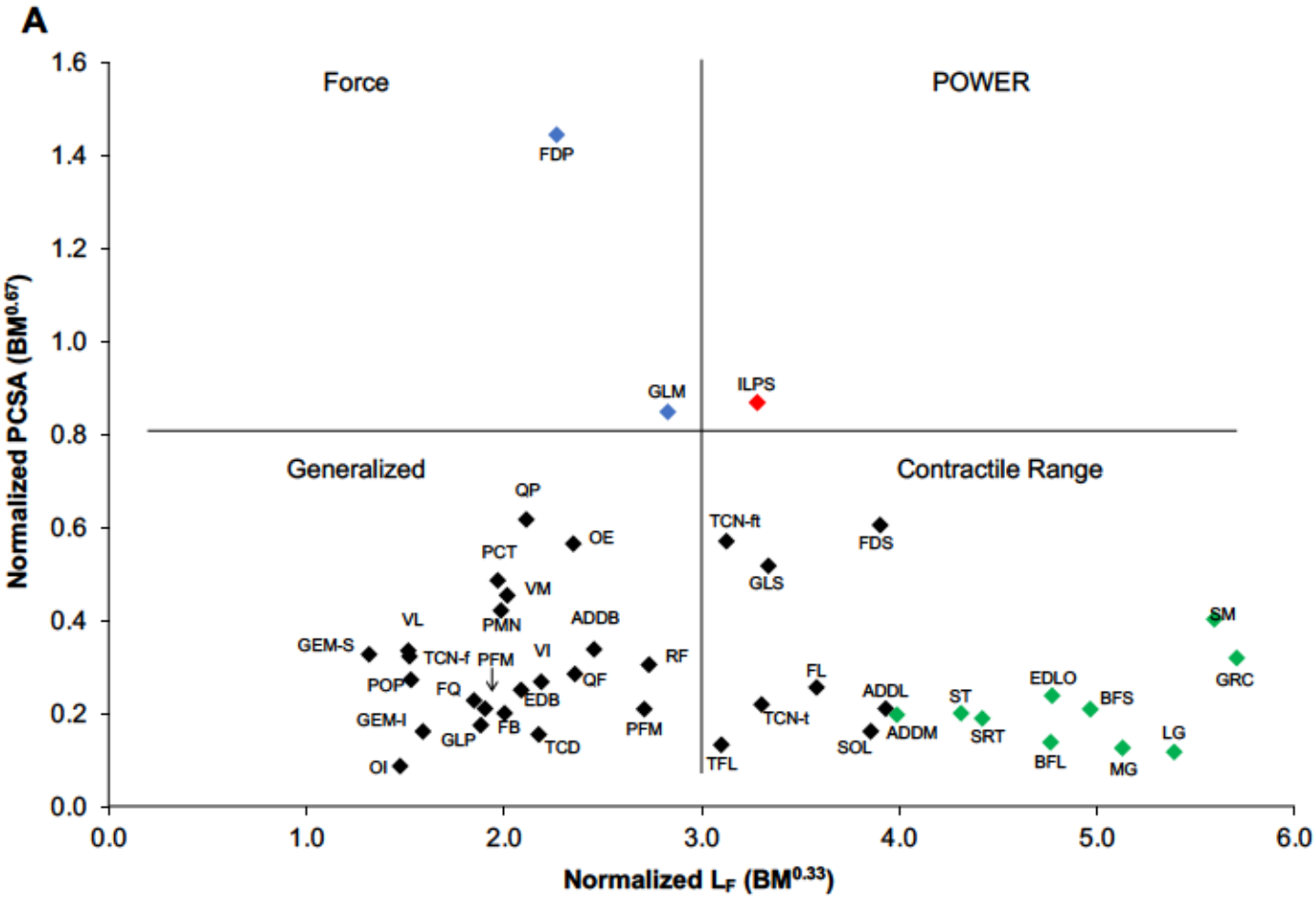
A
Force
POWER
Generalized
Contractile Range
FDP
GLM
ILPS
QP
OE
PCT
VM
PMN
VL
ADDB
GEM-S
TCN-f
PFM
VI
RF
POP
FQ
QF
EDB
GEM-I
GLP
FB
TCD
PFM
OI
TCN-ft
FDS
GLS
FL
ADDL
TCN-t
SOL
ADDM
TFL
ST
SRT
EDLO
BFS
BFL
LG
MG
SM
GRC
Normalized PCSA (BM0.67)
Normalized LF (BM0.33)
0.0
0.2
0.4
0.6
0.8
1.0
1.2
1.4
1.6
0.0
1.0
2.0
3.0
4.0
5.0
6.0

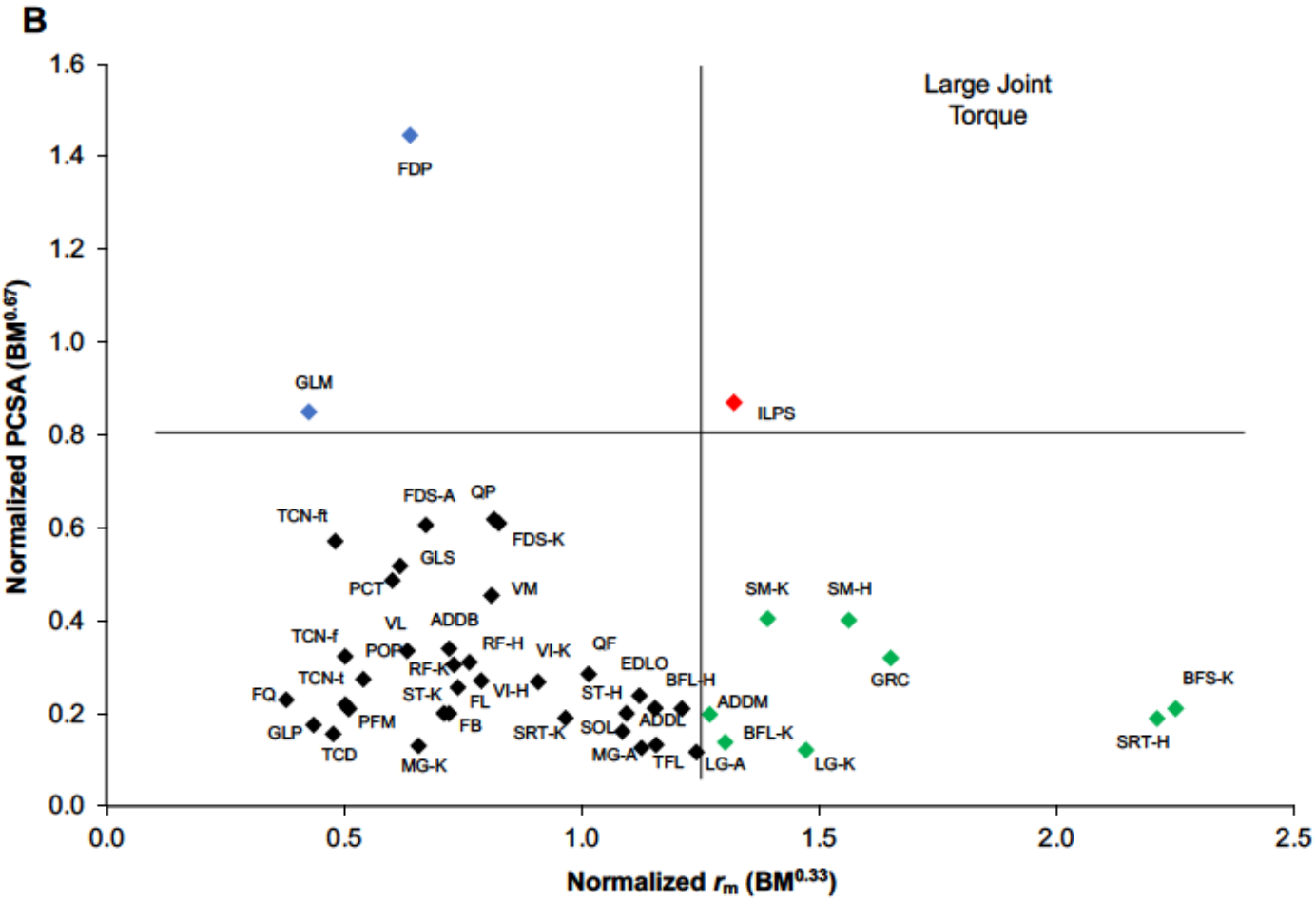
B
Large Joint Torque
FDP
GLM
ILPS
FDS-A
QP
TCN-ft
FDS-K
GLS
PCT
VM
SM-K
SM-H
VL
ADDB
TCN-f
RF-H
VI-K
QF
POP
RF-K
EDLO
GRC
BFS-K
TCN-t
BFL-H
FQ
ST-K
FL
VI-H
ST-H
ADDM
PFM
ADDL
GLP
FB
SRT-K
SOL
BFL-K
SRT-H
TCD
MG-K
MG-A
TFL
LG-A
LG-K
Normalized PCSA (BM^0.67)
Normalized r_m (BM^0.33)
0.0
0.2
0.4
0.6
0.8
1.0
1.2
1.4
1.6
0.5
1.5
2.0
2.5

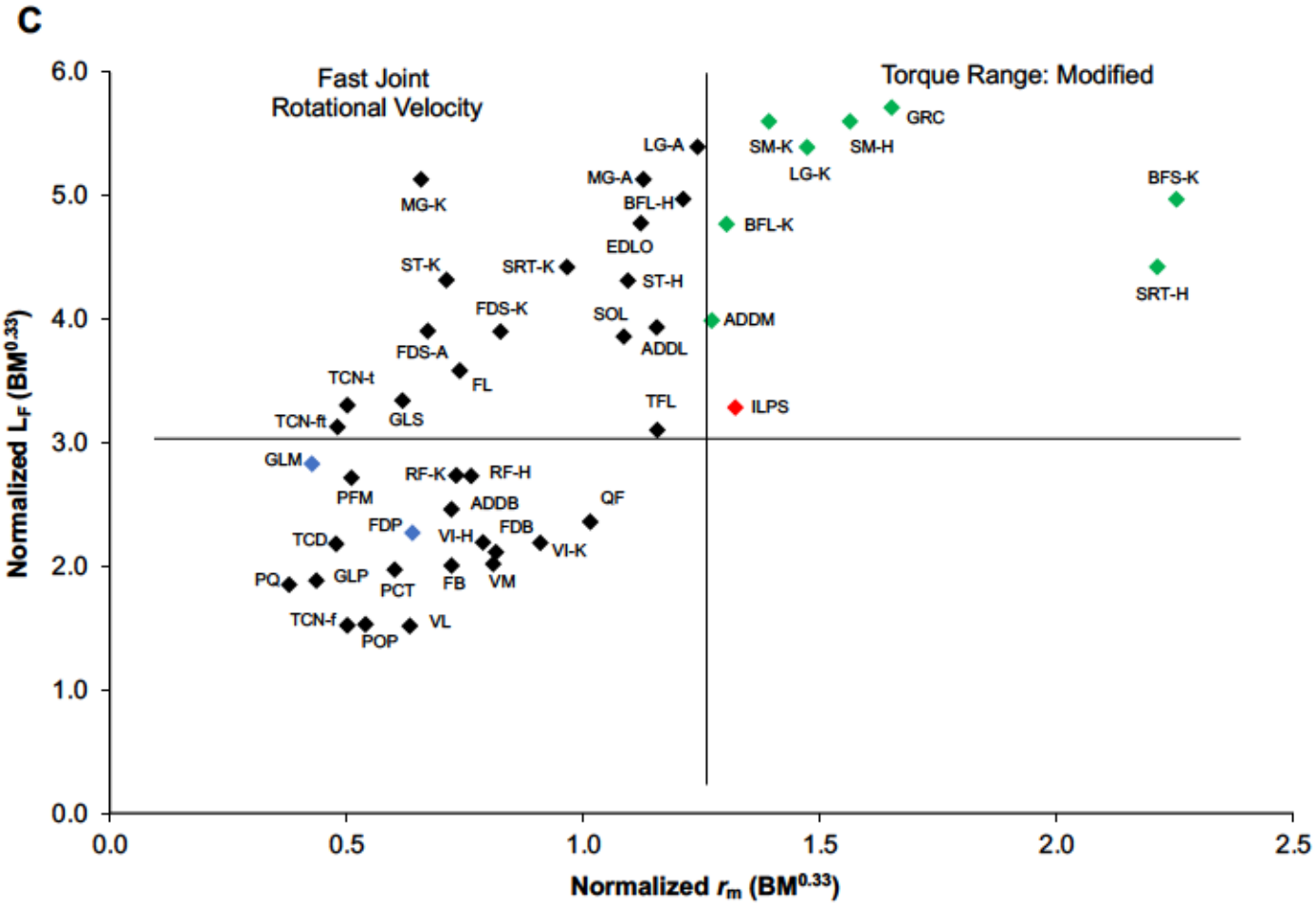
C
Fast Joint
Rotational Velocity
Torque Range: Modified
Normalized L_F ($BM^{0.33}$)
Normalized r_m ($BM^{0.33}$)
6.0
5.0
4.0
3.0
2.0
1.0
0.0
0.0
0.5
1.0
1.5
2.0
2.5
GRC
SM-K
SM-H
LG-K
LG-A
MG-A
BFS-K
MG-K
BFL-H
BFL-K
EDLO
ST-K
SRT-K
ST-H
SRT-H
FDS-K
SOL
ADDM
FDS-A
ADDL
TCN-t
FL
TFL
ILPS
TCN-ft
GLS
GLM
RF-K
RF-H
PFM
ADDB
QF
FDP
VI-H
FDB
TCD
VI-K
PQ
GLP
PCT
FB
VM
TCN-f
VL
POP

Fig 3 Architectural index of fascicle length (L_F) to muscle length (ML) for muscles in the hindlimb of *B. variegatus*. Some muscles are measurements from a single individual, otherwise *bars* are means±s.d. (N=7) and are color-coded by limb region. High mean ratios (>0.6–0.7) indicate substantial shortening capability and velocity of contraction. Muscle abbreviations (as defined in Table 1): ILPS, iliopsoas; PMN, psoas minor; TFL, tensor fascia latae; GLS, gluteus superficialis; GLM, gluteus medius; GLP, gluteus profundus; PFM, piriformis; GEM-S, superior gemellus; GEM-I, inferior gemellus; QF, quadratus femoris; OE, obturator externus; OI, obturator internus; SRT, sartorius; GRC, gracilis; PCT, pectineus; ADDB, adductor brevis; ADDL, adductor longus; ADDM, adductor magnus; ST, semitendinosus; SM, semimembranosus; BFL, biceps femoris long head; BFS, biceps femoris short head; RF, rectus femoris; VI, vastus intermedius; VL, vastus lateralis; VM, vastus medius; MG, medial gastrocnemius; LG, lateral gastrocnemius; SOL, soleus; POP, popliteus; FDS, flexor digitorum superficialis; FDP, flexor digitorum profundus; TCD, tibialis caudalis; FL, fibularis longus; FB, fibularis brevis; FQ, fibularis quartus; EDLO, extensor digitorum longus; TCN-t, tibialis cranialis tibial head; TCN-ft, tibialis cranialis fibular et tibial head; TCN-f, tibialis cranialis fibular head; QP, quadratus plantae; EDB, extensor digitorum brevis.

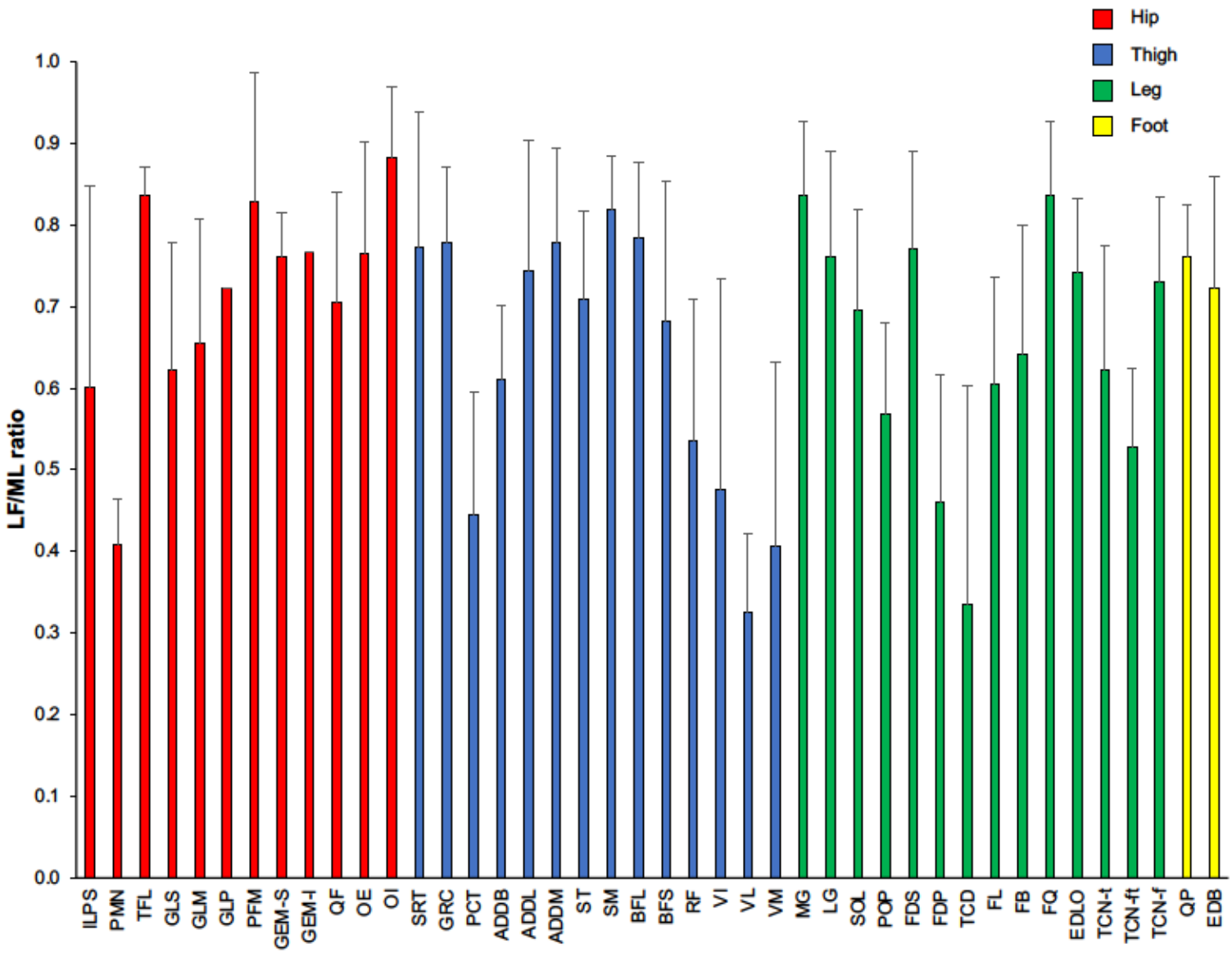
Hip
Thigh
Leg
Foot
LF/ML ratio
1.0
0.9
0.8
0.7
0.6
0.5
0.4
0.3
0.2
0.1
0.0
ILPS
PMN
TFL
GLS
GLM
GLP
PFM
GEM-S
GEM-I
QF
OE
OI
SRT
GRC
PCT
ADDB
ADDL
ADDM
ST
SM
BFL
BFS
RF
VI
VL
VM
MG
LG
SOL
POP
FDS
FDP
TCD
FL
FB
FQ
EDLO
TCN-t
TCN-ft
TCN-f
QP
EDB

Fig 4 Architectural index of physiological cross-sectional area (PCSA) to muscle mass (MM) for muscles in the hindlimb of *B. variegatus*. Some muscles are measurements from a single individual, otherwise *bars* are means±s.d. (*N*=7) and are color-coded by limb region. High mean ratios (>0.5) indicate large force production capability (per unit mass). Muscle abbreviations are defined in Table 1 and are the same used in Figure 3.

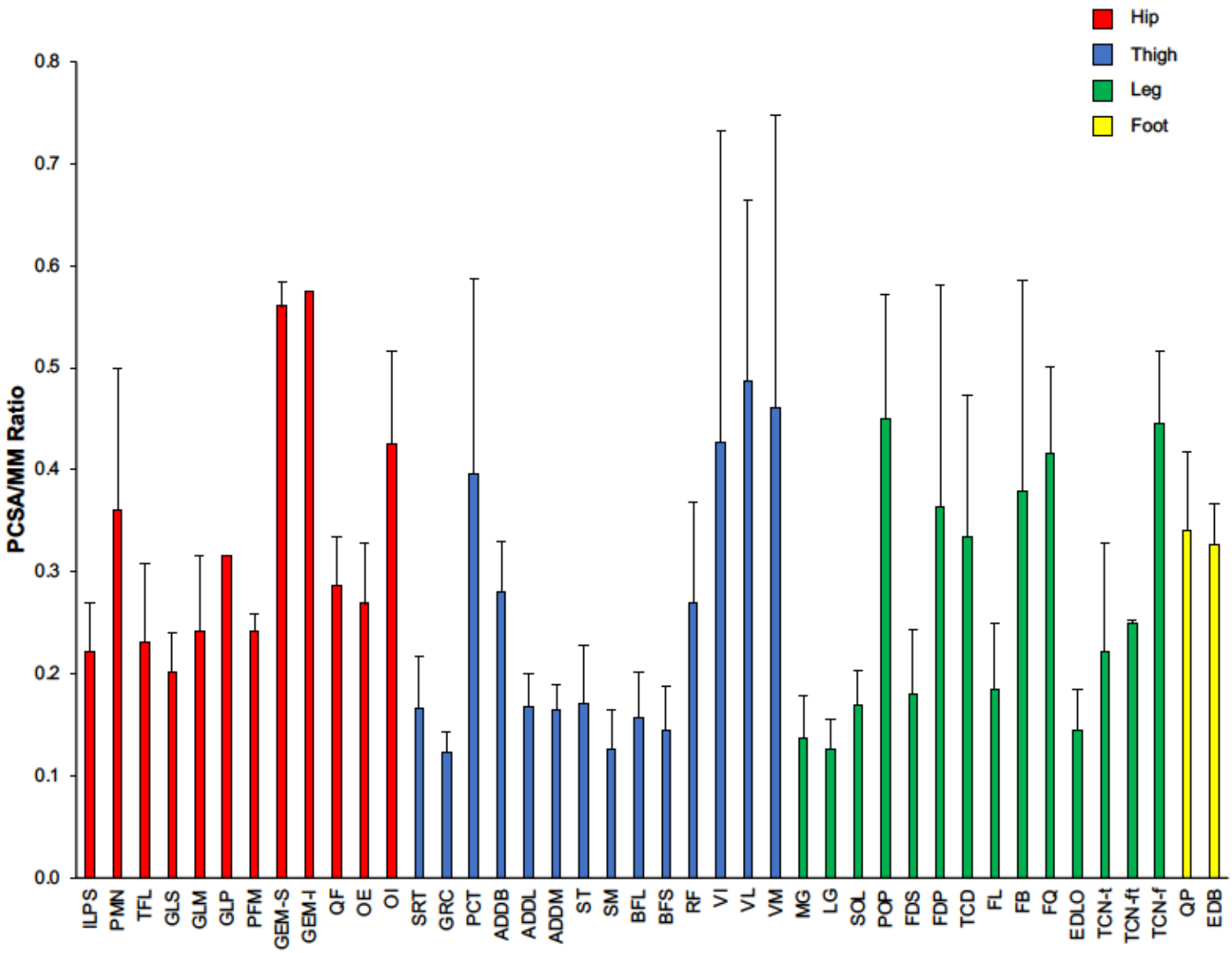
Hip
Thigh
Leg
Foot
PCSA/MM Ratio
0.0
0.1
0.2
0.3
0.4
0.5
0.6
0.7
0.8
ILPS
PMN
TFL
GLS
GLM
GLP
PFM
GEM-S
GEM-I
QF
OE
OI
SRT
GRC
PCT
ADDB
ADDL
ADDM
ST
SM
BFL
BFS
RF
VI
VL
VM
MG
LG
SOL
POP
FDS
FDP
TCD
FL
FB
FQ
EDLO
TCN-t
TCN-ft
TCN-f
QP
EDB

Fig 5 Architectural index of fascicle length (L_F) to muscle moment arm length (r_m) for selected muscles in the hindlimb of *B. variegatus*. Some muscles are measurements from a single individual, otherwise *bars* are means±s.d. (N=6) and are color-coded by limb region. Mean ratios greater than 2–3 (dashed line) indicates an ability for muscle contraction to move the joint through a large range of motion. Designations of H (hip), K (knee), and A (ankle) for bi-articular muscles acting at the hip joint, knee joint, and ankle joint, respectively. Otherwise, muscle abbreviations (as defined in Table 1) match those in Figs. 3 and 4: ILPS, iliopsoas; TFL, tensor fascia latae; GLS, gluteus superficialis; GLM, gluteus medius; GLP, gluteus profundus; PFM, piriformis; QF, quadratus femoris; SRT, sartorius; GRC, gracilis; PCT, pectineus; ADDB, adductor brevis; ADDL, adductor longus; ADDM, adductor magnus; ST, semitendinosus; SM, semimembranosus; BFL, biceps femoris long head; BFS, biceps femoris short head; RF, rectus femoris; VI, vastus intermedius; VL, vastus lateralis; VM, vastus medius; MG, medial gastrocnemius; LG, lateral gastrocnemius; SOL, soleus; POP, popliteus; FDS, flexor digitorum superficialis; FDP, flexor digitorum profundus; TCD, tibialis caudalis; FL, fibularis longus; FB, fibularis brevis; FQ, fibularis quartus; EDLO, extensor digitorum longus; TCN-t, tibialis cranialis tibial head; TCN-ft, tibialis cranialis fibular et tibial head; TCN-f, tibialis cranialis fibular head; QP, quadratus plantae.

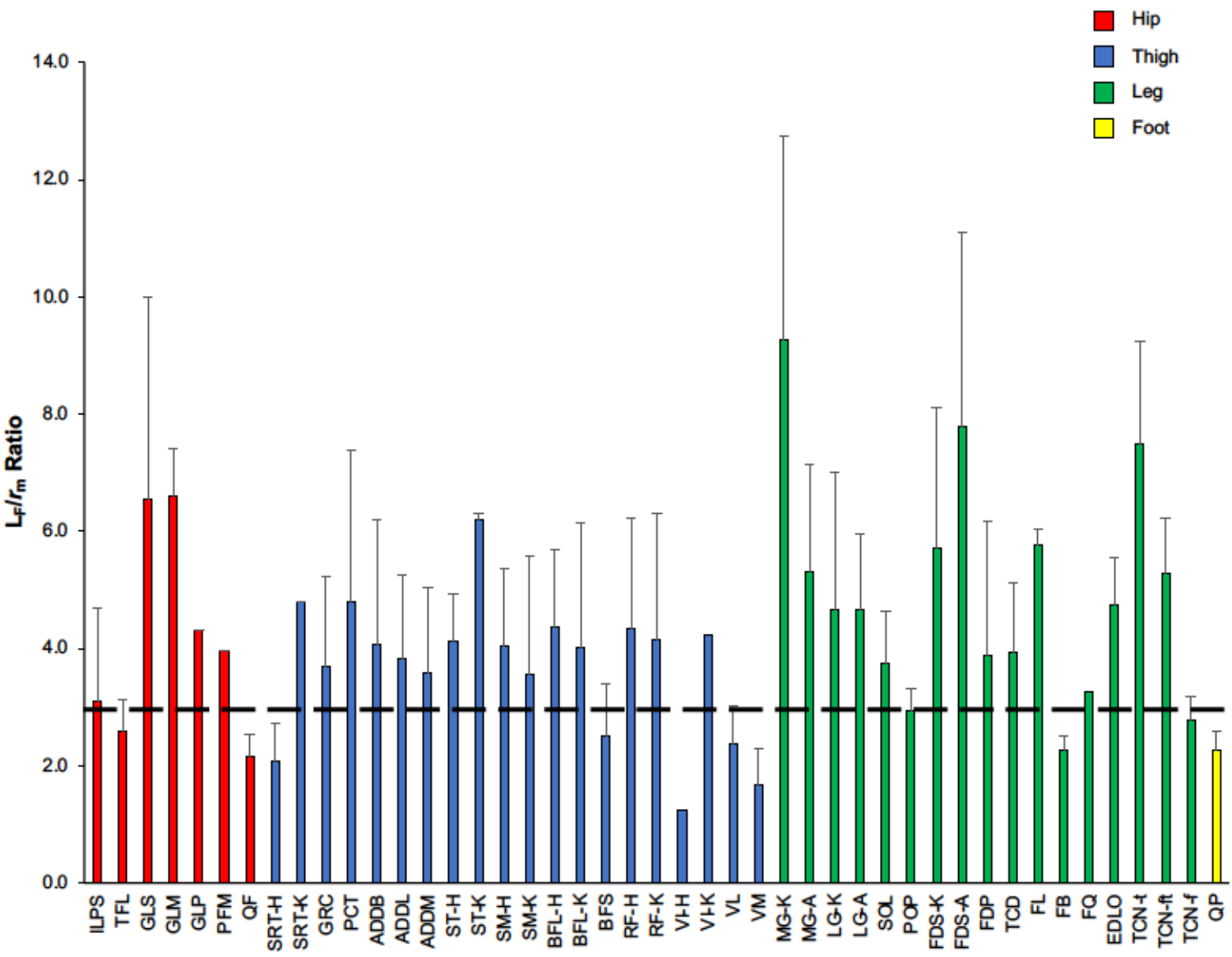
Hip
Thigh
Leg
Foot
L_f/r_m Ratio
14.0
12.0
10.0
8.0
6.0
4.0
2.0
0.0
ILPS
TFL
GLS
GLM
GLP
PFM
QF
SRT-H
SRT-K
GRC
PCT
ADDB
ADDL
ADDM
ST-H
ST-K
SM-H
SM-K
BFL-H
BFL-K
BFS
RF-H
RF-K
VI-H
VI-K
VL
VM
MG-K
MG-A
LG-K
LG-A
SOL
POP
FDS-K
FDS-A
FDP
TCD
FL
FB
FQ
EDLO
TCN-t
TCN-ft
TCN-f
QP

Fig. 6 Statistical comparisons of average MM (**A**), r_m (**B**), L_F (**C**), and total PCSA (**D**) across functional groups and joints in the hindlimb of *B. variegatus*. Flexors at the hip, knee and ankle joints are shown as solid *bars*, whereas the extensors are shown as open *bars*. The functional groups include hip flexors (N=7 muscles), hip extensors (N=6), knee flexors (N=10), knee extensors (N=4), ankle flexors (N=5) and ankle extensors (N=5). Arrows indicate differences between/within flexor and extensor muscle groups at each joint; one asterisk $p<0.05$; two asterisks $p<0.01$; three asterisks $p<0.001$.

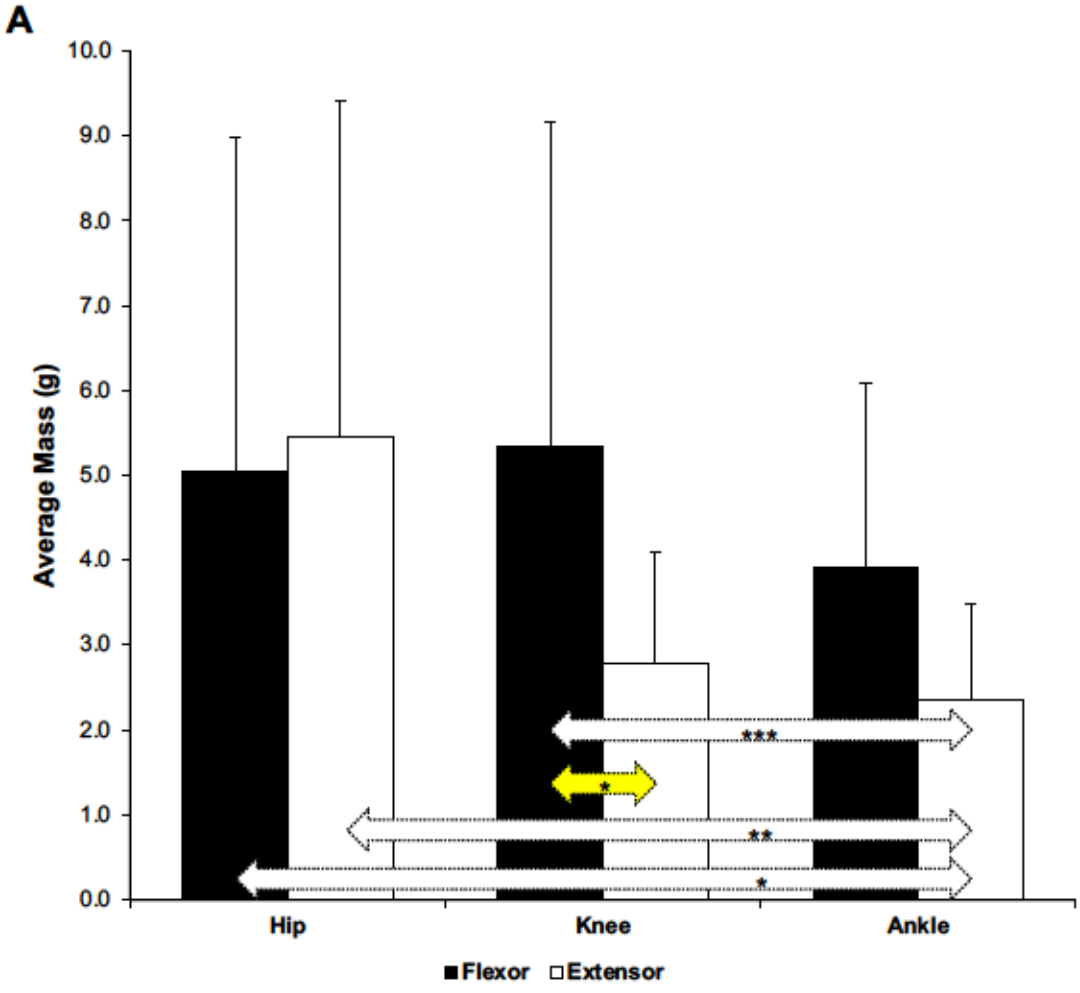
A
10.0
9.0
8.0
7.0
6.0
5.0
4.0
3.0
2.0
1.0
0.0
Average Mass (g)
***
*
**
*
Hip
Knee
Ankle
Flexor
Extensor

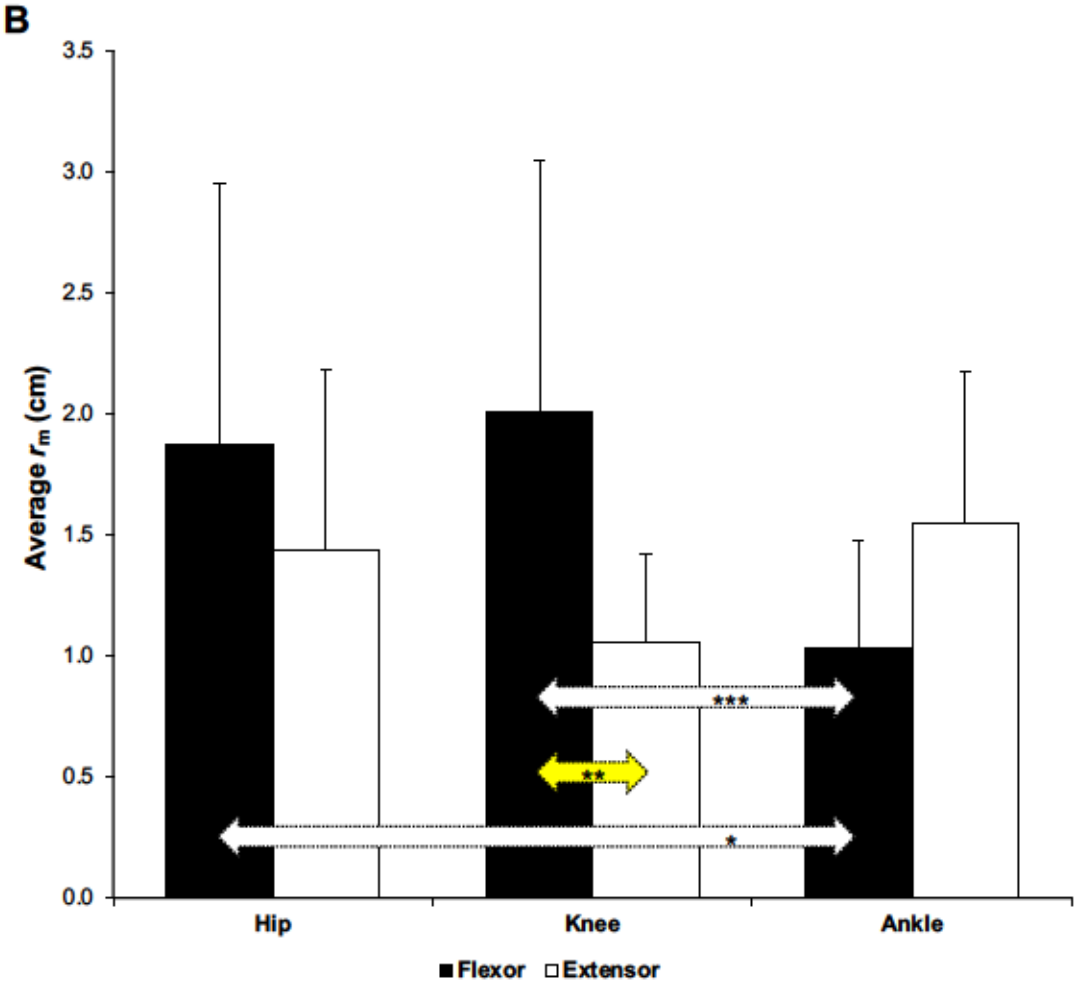
B
3.5
3.0
2.5
2.0
1.5
1.0
0.5
0.0
Average r_m (cm)
***
**
*
Hip
Knee
Ankle
Flexor
Extensor

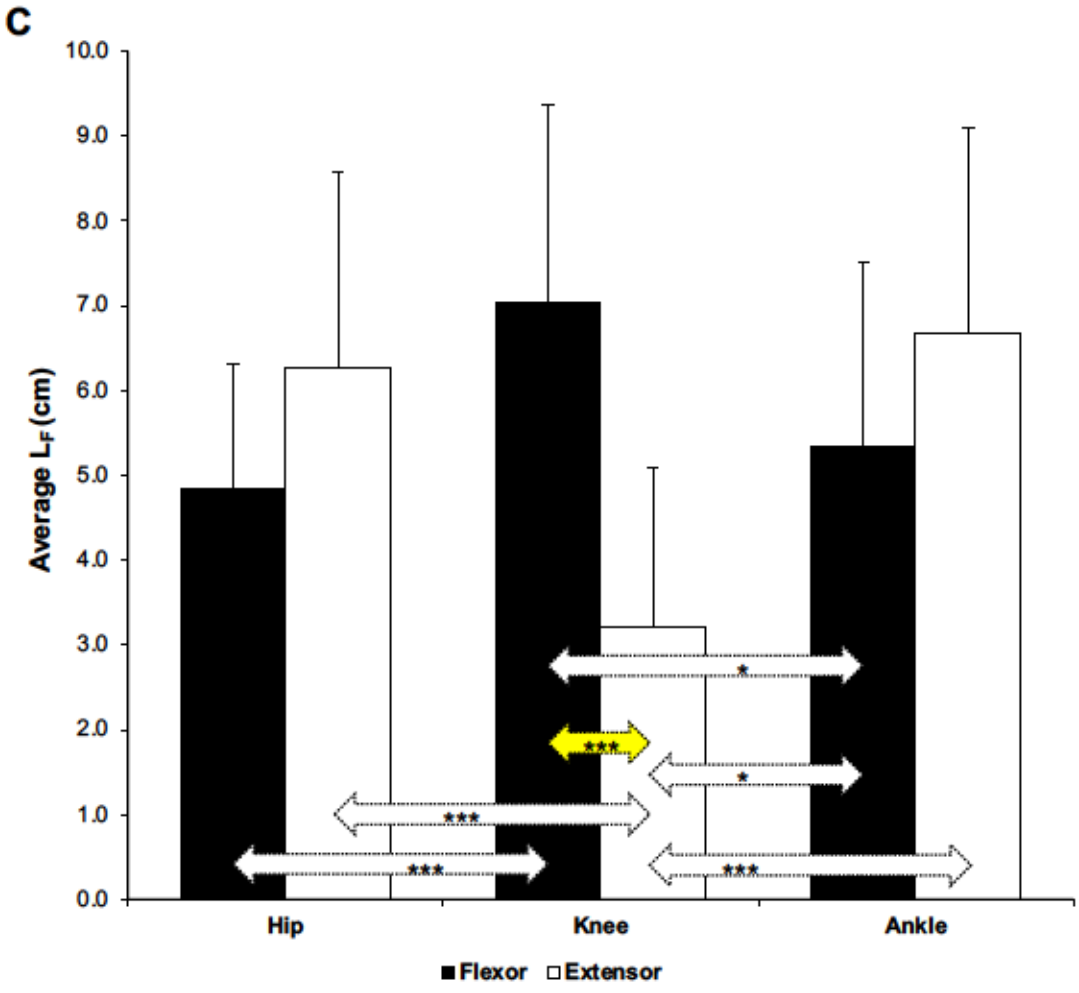
C
10.0
9.0
8.0
7.0
6.0
5.0
4.0
3.0
2.0
1.0
0.0
Average L_F (cm)
*
***
*
***
***
***
Hip
Knee
Ankle
Flexor
Extensor

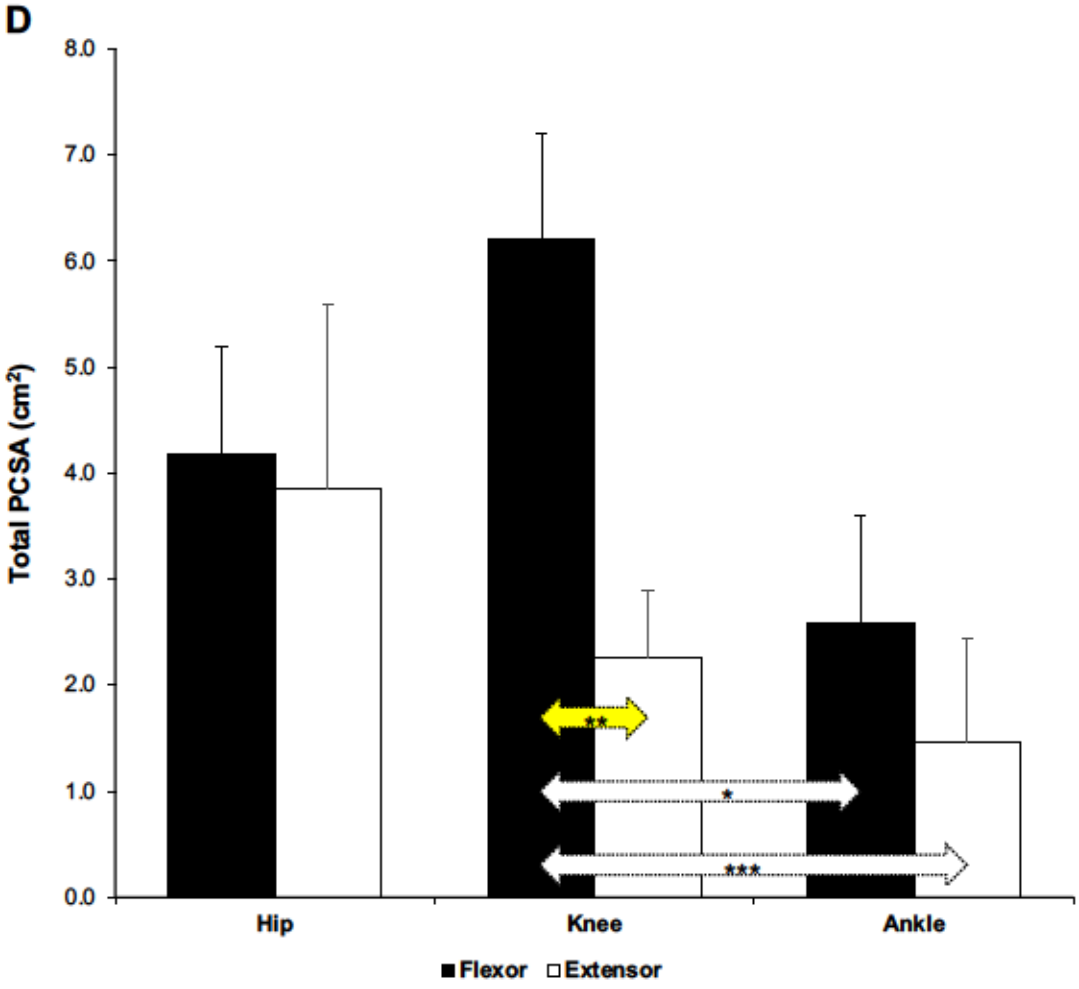
D
8.0
7.0
6.0
5.0
4.0
3.0
2.0
1.0
0.0
Total PCSA (cm²)
**
*
***
Hip
Knee
Ankle
Flexor
Extensor

APPENDIX

Evolution and Speciation

Xenarthra is a superorder of mammals endemic to the modern-day continent of South America. It consists of the orders Cingulata (Armadillos) and Pilosa (Sloths and Anteaters) (Gardner, 2008). The order Pilosa split nearly 40 million years ago into the suborders Folivora (Tree Sloths) and Vermilingua (Anteaters) (Gardner, 2005). The Folivora is further branched into two clades composed of the modern families of 'tree sloths,' Megalonychidae (two-toed sloths) and Bradypodidae (three-toed sloths) (Gaudin, 2004). There are two extant species of two-toed sloths (Genus: Choloepus): *Choloepus didactylus*, or the Linnaeus's two-toed sloth, and *Choloepus hoffmannii*, or Hoffmann's two-toed sloth, whereas there are four extant species of three-toed sloths (Genus: Bradypus). These include the pygmy three-toed sloth (*Bradypus pygmaeus*), maned three-toed sloth (*Bradypus torquatus*), pale-throated three-toed sloth (*Bradypus tridactylus*), and brown-throated three-toed sloth (*Bradypus variegatus*).

Understanding of sloth phylogeny has recently been – and continues to be – revised by a series of molecular studies, based on collagen and mitochondrial DNA sequences (e.g., Presslee et al., 2019). These investigations consistently place the relationship of extant two-toed sloths close to the extinct mylodonts and megalonychids. However, the three-toed sloths are placed within the order Megatherioidea, the extinct linage of giant ground sloths. Megatherioids (e.g., *Megatherium americanum*) once inhabited the Central America regions of the North American Continent where modern tree three-toed sloths are populous today. Moreover, the predominant findings of the genomic studies, in addition to multiple morphological analyses in xenarthrans (see below), provide strong support for the hypothesis that arboreality arose separately in the two genera of modern tree sloths via the process of convergence (Presslee et al., 2019). Therefore, *Choloepus* and *Bradypus* are very distant relatives and evolved their suspensory behaviors independently, making these unusual mammals one of the most remarkable known examples of convergent evolution (Nyakatura, 2012).

Xenarthrans share a number of distinct morphological traits: 1. transverse processes of anterior caudal vertebrae are fused to the pelvis; 2. all species have xenarthrous or 'extra' zygapophyseal joints in their lumbar vertebrate in order to provide enhanced stability to

the trunk; 3. scapula contains a well-developed secondary spine; and 4. palatine vacuities (i.e., an incomplete septo-maxilla) may be present in the roof of the mouth. Additional features that xenarthrans may share include robust skeletons (e.g., armadillos and anteaters: Vizcaíno et al., 2008; Vizcaíno, 2009) and rudimentary teeth (e.g., armadillos and sloths), whereas the anteaters lack teeth in their jaws in favor of a specialized tongue for foraging on ants and termites (Gaudin and McDonald, 2008; Gaudin and Croft, 2015). Moreover, incisors and true canine teeth of extant sloths (except *Choloepus*) are absent (Pujos et al., 2012). Last, xenarthrans as an entire Superorder are also well known to have lower basal metabolism, lower body temperatures, and slower digestion rates in comparison to other placental mammals (Sunquist and Montgomery, 1973).

Ecology and Physiology

Extant sloths are found in the neotropical rainforests of Central and South America (Britton, 1941). The species *C. hoffmanni* is found in two disjunct areas. The northern population ranges from Honduras and Nicaragua to western Venezuela, and the southern population ranges from north-central Peru through southwestern Brazil to central Bolivia (Hayssen, 2011). The species *B. variegatus* is distributed north in Nicaragua, Honduras, Ecuador, Colombia, Venezuela, and extends further south than *C. hoffmanni* into Brazil and northern Argentina. On average, *C. hoffmanni* has a larger home range of 1.97 hectares compared to the 1.59 hectares for *B. variegatus* (Montgomery and Sunquist, 1975). These distributions do overlap causing sympatry, primarily in the northern regions (e.g., Central America) of the geographic range, but species are disparately separated in southern regions (Hayssen, 2010).

Sloths are high canopy folivores whose diets are of low nutritional (energy) value, consisting primarily of leaves (Montgomery, 1983). However, there are differences between the diets of both genera correlating with the native vegetation within regions of their home ranges. Notably, *Bradypus* is restricted to consumption of leaves from fifteen species of Cecropia trees (e.g., Gauramo), while *Choloepus* has a more diverse diet, including buds, flowers, fruits, and twig tips from 34 species of Cecropia trees (Meritt,1985; Montgomery, 1983; Vaughn, 2007). Sloths descend their home trees an average of every 4–8 days to defecate (Voirin et al. 2013). However, sloths are most vulnerable being on the forest floor. This is because a variety of carnivorous animals

including anacondas, margays, ocelots, and jaguars all have a greater opportunity to prey on sloths during, but not limited to this period in time (Garla, et al., 2001; Touchton et al., 2002). Jungle cats such as margays and ocelots are strong and capable of ascending trees to the level of the canopy, while hawks and harpy eagles (native to the neotropics) can detect a prey sloth from a position above the emergent tree line.

Sloths have little ability to evade predators and are essentially defenseless when on the forest floor. Interestingly, a contrast in tree descent is observed between *Choloepus* and *Bradypus*, and this pattern of movement is potentially due to predation avoidance strategies related to both their mobility and a stronger sense of either sight or smell. For example, *B. variegatus* has a tail first descent, which may be due to its ability to rotate the head 180° (total range of motion: 270°, see below) in order to scan the surrounding area for any predators. The mobility of the head further relates to a reliance on sight in *Bradypus*. Sloths generally have poor eyesight, but it is suspected that three-toed sloths have better visual acuity than two-toed sloths (Mendel 1985a). On the other hand, *C. hoffmanni* descends trees headfirst, and this could be related to its reliance on sense of smell for threat detection. *Choloepus* demonstrates more overt (and threatening) defensive behavior than *Bradypus*, and these include forelimb claw slashing, hissing, and baring teeth. While *B. variegatus* may try to thwart an avian predator (e.g., harpy eagle) in the canopy with some slashing gestures, its main predatory defense strategy is stealth and/or camouflage (Enders 1935; Montgomery and Sunquist, 1978; Mendel, 1985a). When attacked by a predator, *Bradypus* clings strongly to the substrate or may try to grasp onto the predator to pierce its flesh with their long, sharp foreclaws.

Slow, deliberate movement patterns are not only linked to predator avoidance, but also reflect an energy poor diet. Sloths have a low daily food intake an average of 17g dry weight per day, which is related to their low metabolic rates (Cliffe et al., 2015, 2018). For example, *B. variegatus* has the lowest recorded field metabolic rate (162 kJ/day*kg^0.734) among non-hibernating mammals (Pauli et al., 2016). Sloths also have unusually low body temperatures for placental mammals, averaging only 32.7°C in *Bradypus* and 34.5°C in *Choloepus* (Pauli et al., 2016). In addition, adult *B. variegatus* has a smaller body mass range of 3.2–6.1 kg while that for *C. hoffmanni* is larger, averaging 7.0–9.0 kg (Genoways and Timm, 2003; Gillespie, 2003), and differences in

body size can be correlated with differences in body temperature and thermoregulatory strategies of sloths. Thus, their overall low body temperatures further indicates that they are heterothermic and must employ behavioral thermoregulation to conserve metabolic energy to cope with daily temperature fluctuations and diurnal versus nocturnal activity observed in different species of sloths (Cliffe et al., 2018). The species *B. variegatus,* for instance, will employ sun basking for warmth atop the canopies during the early morning hours, and they descend into the canopy shade as the temperature rise throughout the day (Montgomery and Sunquist, 1978). In contrast, *C. hoffmanni* does not prefer the canopy and emergent levels of rainforest vertical strata and mainly occupies the understory to canopy level in the trees and tends to be more active at night (see below) when temperatures are cooler. Having larger body mass means that two-toed sloths have a smaller surface area to volume (SA: V) ratio and can more easily retain body heat for internal warmth.

In addition, different patterns of wakefulness are observed among species of sloths. *Bradypus* is diurnal meaning it is active both during day and night but spends 15–18 hours a day resting and/or sleeping (Sunquist and Montgomery, 1973). Also, *B. variegatus* is reported to have several modes of sleep/wake cycles including (a) "awake-exploring" where the animal is alert, moving the head, and blinking frequently, (b) "awake-alert" where the head is up and eyes open, blinking occasionally, (c) "awake-fixating" where the head is up and eyes open, but the animal shows a tonic immobility, (d) "behavioral sleep" where the animal sits in a reclined position (in a branch recess-elbow) with its head tucked or suspends (i.e., hangs) beneath a tree branch with its head down and eyes closed (Barratt, 1965). In contrast, *C. hoffmanni* is primarily nocturnal, being active ~11 hours during the night and sleeping beneath the canopies of trees during the day (Montgomery et al., 1973; Montgomery and Sunquist, 1975). The activity patterns of both genera demonstrate that sloths are not highly active animals, thereby reinforcing the supposition that their behavior, as well as their physiology, is correlated and modified in extreme ways to conserve metabolic energy (Cliffe et al., 2018).

Locomotion and Gait Patterns

Sloths evolved a below-branch (anti-pronograde) mode of locomotion making them one of a few taxa of mammals for which suspensory locomotion and posture is nearly

obligatory. Average velocity for suspensory walking in sloths was originally reported to be ~0.14 ms^{-1} (Britton and Atkinson, 1938). A recent study (Gorvet et al., 2020) found that *B. variegatus* moves even slower (0.07 ms^{-1}) beneath a beam when allowed to freely choose their preferred speed, whereas velocities in *C. didactylus* have been reported to be considerably greater than these averages in studies using treadpoles for steady-state measurements (Nyakatura et al., 2010). Despite differences in absolute speeds, both species exhibit a lateral sequence diagonal-couplet (LSDC) gait (Cartmill et al., 2002; Usherwood and Davies, 2017) during suspensory walking but use a diagonal sequence gait with near diagonal couplets during vertical climbing. These patterns were most definitely determined by the recent work of Gorvet et al. (2020). Briefly, a diagonal-sequence gait is defined by consecutive footfalls (or grips onto a substrate) of contralateral fore- and hindlimb pairs (Muybridge, 1887; Hildebrand, 1985). A diagonal couplet is specifically a pattern of footfalls whereby contralateral pairs of feet (fore- and hindfeet) contact the substrate simultaneously (Hildebrand, 1985; Mendel, 1985a).

Diagonal-sequence gaits are most often employed by mammals (e.g., primates) that use above branch (pronograde) locomotion for stability on arboreal substrates. The diagonal pattern of footfalls prevents rolling off (via a large rolling torque) of branches that would otherwise occur by bearing the majority of weight on one side of the body as during a lateral sequence gait. Although sloths can perform both arboreal and terrestrial locomotion (akin to a crawl), they do not demonstrate a running gait during either mode of transport (Mendel, 1981a, 1985). Moreover, whereas brachiating primates (e.g., gibbons and siamangs) use to pendular mechanics via arm swinging to locomote and reduce metabolic cost (Bertram and Chang, 2001), such mechanics are not available to sloths. In contrast, sloths must move in a manner that minimizes fluctuations of the dynamic forces exerted on the support (Nyakatura and Andrada, 2013) so as not to make the support unstable or oscillate, thereby not creating wasted effort when walking but they cannot swing of take advantage of pendulum-like energy exchanges.

Another important distinction between pronograde versus anti-pronograde locomotion is that joint torques in upright quadrupeds reflect the need to counteract gravitational induced flexion of the limb (i.e., limb loading). Thus, the limb extensor muscles of pronograde arboreal mammals have an anti-gravity role to prevent limb collapse during

weight bearing (Cohen and Gans 1975; Jenkins and Weijstouch, 1979). However, since locomotion and posture in sloths is of the inverse orientation, gravitational induced extensor torques at the limb joints must be controlled by limb flexor muscles (Fujiwara et al., 2011). An anti-gravity role in the elbow of suspensory mammals has indeed been experimentally shown (see below) for brachiating primates and in lorisids that use suspensory locomotion as well as slow, intermittent movement patterns (Jungers and Stern 1980, 1981; Jouffroy and Stern, 1990). The slow and deliberate locomotion of sloths (e.g., 0.07 ms^{-1}: Gorvet et al., 2020; 0.02–0.47 ms^{-1}: Nyakatura et al., 2010; 0.04–0.19 ms^{-1}: Granatosky et al., 2018) is emphasized when compared with higher speeds of agile primates that employ facultative suspensory locomotion, but primarily locomote above branch, including the grey mouse lemur (0.39–0.89 ms^{-1}) and squirrel monkey (0.39–1.00 ms^{-1}) (Schmidt, 2008), as well as the slow loris (0.73 ms^{-1}; Schmitt and Lemelin, 2004).

Functional Morphology, Myology, and Muscle Physiology

Sloths have notably reduced skeletal muscle mass for mammals. The skeletal muscle mass of sloths comprises only 23.6% of total body mass for *B. variegatus* and 26.2–27.4% for *C. hoffmanni* (Grand, 1978). For comparison, other arboreal mammals have an average skeletal muscle mass of ~33% their total body mass (Muchlinski et al., 2012). These data indicate that a reduction in muscle mass is representative of an adaptation for arboreal lifestyle. Other morphological features are somewhat unique (among mammals) to sloth form and include modifications to the neck and pectoral girdle as well as their feet. For example, *B. variegatus* notably has 8-9 cervical vertebrae, allowing for exaggerated rotation of the head up to 180° (in a cranial-caudal orientation), hence the ability to look forward while suspended below-branch (Mendel, 1985a). *Choloepus*, on the other hand, has only 5-6 cervical vertebrae, which limits the rotation of the head/neck, and places more emphasis on hyperextension of the neck as the functional motion while in a suspensory posture. Whereas the unusual number of cervical vertebrae is a main example of the distinct morphology in sloths, it is also one of prominent differences between two-toed and three-toed forms. Additionally, *B. variegatus* has forelimbs that are longer than their hindlimbs and has a reduced tail. In contrast, *C. hoffmanni* has fore and hindlimbs that are elongate and of equal length and it lacks a tail (Britton, 1941). The

differences in limb length are further evidence that indicates the ecological preferences among species. In this case, *C. hoffmanni* prefers a support that is parallel to the ground, and although *Choloepus* spends more time in suspension than *Bradypus*, both genera independently evolved a suite of adaptations that allow for their arboreal and suspensorial lifestyle.

The structural requirements for suspension involve those of a tensile limb system. Sloths have modified pelvic and pectoral girdles with hip/shoulder joints that are able to support their limbs loaded in tension rather than in compression. In order for the pectoral girdle to efficiently rotate from a dorsal to more lateral position, the scapulae of both genera are reduced in size, and the thorax is reduced cranially and has a circular cross-section. In addition, sloths have a ligament of fibrous connective tissue that connects the clavicle to the sternum, which permits greater degrees of freedom for rotation at the sternoclavicular articulation (Nyakatura and Fischer, 2010). Evidence suggests that the greatest torque (or moment) occurs at the thoraco-scapular articulation and shoulder joint when the forelimb touches down during suspensory walking with the moment reaching nearly 1Nm/kg in magnitude. Therefore, the center-of-mass (CoM) does not accelerate, which allows the movement to be slow, controlled and the CoM is translated forward in a uniform manner (Nyakatura and Andrada, 2013). The forelimb flexor muscles of sloths must then provide support of their body weight at the digital/carpal, elbow, and shoulder joints by some combination of active and/or passive means (via tensile loading) much like that observed in primates with suspensory habits (Granatosky et al., 2018). While tensile loading of distal flexor tendons and their muscle-tendon units (MTU) with adequate stiffness could be a major means of body weight support (Mendel 1981a, b; Mendel, 1985), activation of strong elbow flexors in sloth forelimbs likely mitigates levels of limb force (Granatosky et al., 2018; Gorvet et al., 2020), especially loading of the highly mobile shoulder joints in sloths. Overall, function of their tensile limb system (see below) is expected to reduce muscular recruitment (i.e., volume of active muscle) during postural suspension (Gorvet et al., 2020) as previously suggested in arboreal primates (Preuschoft and Demes, 1984).

All sloths have highly modified feet. Regardless of the number of digits remaining on their forefeet, all sloths have three digits on their hindfeet. The species *B. variegatus* has

three functional digits on the forefeet that are partially fused – digits II, III, and IV. In general, *Bradypus* (sp.) have vestigial metacarpals I and V, which remain as splint-like bone appendages. Three-toed sloths also have long claws at the end of their curved distal phalanges and have volar pads that are covered with fur. Unlike three-toed sloths, *Choloepus* (sp.) has two function digits on their forefeet – digits II and III. Metacarpals I and IV are vestigial and splint-like in the two-toed sloth condition, with digit V being absent. The species *C. hoffmanni* also has long, recurved claws on their digits, but their volar pads are hairless and have thick, leathery skin. The claws of both genera act as hook-like projections which help them to perform their suspensory locomotion and posture (Mendel, 1981a, b). Moreover, depending on the diameter of the arboreal substrate, *Choloepus* may grip the support mainly with its claws versus *Bradypus* that places a large area of its feet on the substrate. *Bradypus* may also prefer, or cope, with larger diameter supports better than *Choloepus* (Mendel 1981a, b; Mendel, 1985; Granatosky et al., 2018; Gorvet et al., 2020).

Another source of support to the distal limbs in sloths is their flexor tendons, which can serve as a suspensory (or passive-stay) apparatus. Limb tendons in numerous terrestrial mammals are known to function as stiff, elastic elements for joint position control and/or as efficient biological springs during locomotion to conserve energy during running (Alexander, 1984). For example, in horses and other ungulates, MTU are extremely modified to undergo large strain by having long, thin insertion tendons capable of large elastic strain energy storage and recovery (Biewener, 1998). Tensile strain in their MTU may also occur with little-to-no muscle activation, thus the resisting force is passive tension during postural behavior (Lieber, 2002; Hodson-Tole et al., 2016.) Notably, horses have a weight-bearing suspensory apparatus (Hildebrand, 1960) which allows them to remain standing for long periods of time without muscle fatigue (Hermanson and Cobb, 1992). These specializations in distal MTU structure-function reduce metabolic energy expenditure that would otherwise need to be supplied by muscle contraction and work (Biewener, 1998). Sloth flexor tendons demonstrate a functional trade-off between stiffness and compliance to passively support body weight (Mossor et al., in revision), while muscle contraction can modulation tendon stiffness for joint position control translated as a strong grip on the substrate (Gorvet et al., 2020). Indeed,

Mossor et al. (in revision) showed that sloth FDP tendons have low strength and elasticity indicating simplified tendons that have functional properties appropriate for suspensorial habits (opposite of the specialized tendons in cursorial or saltatorial taxa). Moreover, these tendons are not expected to behave as biological springs because sloths cannot run. Energy conservation for passive support and possibly the minimal investment of metabolic energy resources in maintenance of tendon tissue may be representative of a functional suspensory apparatus in sloths (Mossor et al., in revision).

a. Hindlimb Musculature

The musculature of the pelvic (hind) limbs purportedly acts to keep hip (acetabulofemoral) joint stabilized in an extended position and the claws flexed for grip on the substrate. The actions of the respective functional muscle groups (hip extensor/knee flexors and digital flexors) are *a priori* based on the locations of their origin and insertions reported in numerous historical volumes (Humphrey, 1870; Macalister, 1869; Mackintosh 1875a, b; Windle and Parsons, 1899; Wislocki, 1928). This sub-section is not intended to be a thorough review of hindlimb myology (main objective of this study: see below) but instead a summary of muscles and major functional muscle groups. However, where appropriate, individual muscles will be highlighted and detailed.

Hindlimb muscles originating from the hip region should act to protract and retract the femur (or limb) at the hip joint, as well as stabilize the hip joint during suspensory locomotion and posture. The cranial region of the hip joint contains the m. iliacus, m. psoas, m. sartorius, and m. tensor fascia latae (craniolateral) that can act as hip joint flexors. Along the caudal region of the hip joint, the m. gluteus superficialis (caudolateral aspect) should act to both flex the hip and abduct the hindlimb, whereas mm. gluteus medius and gluteus profundus (often inseparable) are positioned to act as the main hip extensors, and secondarily as hindlimb abductors. The m. sartorius is a bi-articular muscle that is expected to not only flex and the abduct femur at the hip joint, but also laterally rotate the thigh and flex the leg at the knee joint. There are five muscles with the potential to adduct the femur at the hip joint, including m. pectineus, m. adductor brevis, m. adductor longus (two heads), m. adductor magnus, and m. gracilis.

Along the cranial and caudal regions of the thigh are located the knee extensors and hip extensor/knee flexors, with the latter collectively called the 'hamstring' muscles. The

quadriceps femoris is composed of four muscle heads: m. rectus femoris, m. vastus intermedius, m. vastus lateralis, and m. vastus medialis. With the exception of m. rectus femoris, which is bi-articular and has a small muscle moment arm at the hip joint, the knee extensors originate from the proximal and/or mid-shaft region of the femur and all heads insert on the tibial tuberosity via the quadriceps tendon containing the patella. The mm. semimembranosus, semitendinosus, and biceps femoris along the caudal thigh are all bi-articular and act in hip extension and knee flexion. Additionally, the two medial muscles m. semimembranosus and m. semitendinosus may internally rotate the leg when the knee is flexed. However, the larger of the two heads of m. biceps femoris (or m. flexor crurus longus) that crosses the hip and knee joints to insert distal onto the crural fascia may act to laterally rotate the hip joint and aid in adduction of the femur.

The muscles of the leg act to flex/extend the leg at the knee or to flex/extend the hindfoot at the ankle, in addition to resisting gravitational extension of both the knee and ankle joints (i.e., anti-gravity muscles). The bi-articular m. gastrocnemius (medial and lateral heads) are superficial muscle bellies along the caudal aspect of the leg and their actions are flexion of the leg at the knee joint and extension of the hindfoot at the ankle joint via the calcaneal tendon. The small m. soleus deep to and inserts in common with the m. gastrocnemius onto the calcaneal tuberosity but acts in only ankle extension. The m. flexor digitorum superficialis is also a bi-articular muscle and superficial to the m. gastrocnemius that inserts onto a robust common flexor tendon that crosses the ankle joint and then gives of three tendon slips, one for insertion onto the terminal phalanx (base of claw) of each digit. The common flexor tendon in the hindlimb arises from the distal bellies of well-developed m. flexor digitorum profundus, which is the deepest muscle of the caudal leg. It is possible that m. flexor digitorum profundus facilitates ankle extension, whereas only the belly m. flexor superficialis can act to flex the knee. Collectively, the m. flexor digitorum profundi is a muscle complex with 4 heads total that provide for strong flexion of the metatarsophalangeal and interphalangeal joints to conform the hindfeet into a hook-like appendage (Nyakatura and Andrada, 2013).

Ankle flexion is the main role of the m. tibialis cranialis (tibial and fibular heads). Ankle flexors also include m. fibularis longus and m. fibularis quartus, while the m. extensor digitorum longus likely facilitates flexion of the ankle joint. Muscles that

perform ankle flexion/extension may also act the pronators and supinators of the hindfoot. For example, mm. fibularis longus and fibularis quartus, as well as m. fibularis brevis, and all act as pronators of the hindfoot, whereas the supinators of the hindfoot include m. tibialis cranialis and m. tibialis caudalis. The m. tibialis caudalis may also act to extend the ankle joint. Lastly, the intrinsic foot musculature is overall reduced due to the loss of digits. The main belly of the plantar aspect of the foot is m. quadratus plantae and it is a flexor of digits II-IV. On the dorsal side of the foot is m. extensor digitorum brevis that facilitates extension of digits II-IV. The mm. interossei are relatively well-developed, and due to the fused state of the metatarsals, they most likely act to flex the metatarsophalangeal joints and proximal interphalangeal joints (Mendel, 1985b), but to a lesser extent, abduct the digits. However, the mm. lumbricals are reduced in *B. variagatus*, where just one (Mendel, 1981) or two (Humphrey, 1870; Windle and Parsons, 1899) bellies were observed, while as many as 4 bellies were previously described in *C. hoffmanni* (Mackintosh, 1875a).

b. Muscle Fiber Architecture

Muscle architecture is defined as the orientation of muscle fibers relative to the axis of force production (Lieber, 2002). There are two main fiber architectures: pennate- and parallel-fibered muscles. Pennate muscles have fascicles (bundles of muscle fibers) that are attached obliquely to the tendon of insertion or a tendinous inscription(s) that run throughout the muscle belly. The angle at which the fascicles are arranged relative to fascial plane or intramuscular tendon tissue is known as pennation angle and this metric typically ranges from 0° to 45° under resting conditions. However, when muscles are recruited to produce active force and perform mechanical work, this causes fibers to rotate about their origin, and thus pennation angle changes as muscles shorten during contraction (Gans, 1982, Azizi et al., 2008). By definition, pennate-fibered muscles have resting pennation angles of 15-45° (Zajac, 1989, 1992). Assessment of muscle architecture properties involves measurement of the resting pennation angle of the fascicles, in addition to fascicle length, muscle belly length, and muscle belly mass. In general, the magnitude of force produced by pennate-fibered muscles is larger than that of parallel-fibered muscles. This is because fiber pennation corresponds with shorter fascicles, which in turn, allows for a greater number of muscle fibers per unit area of

muscle tissue (Gans, 1982, Azizi et al., 2008). Therefore, pennate muscles typically have greater physiological cross-sectional area (PCSA) than parallel-fibered muscles, and PCSA is proportional to the isometric force production capability of muscles (Alexander, 1984; Williams et al., 2008). Pennation then provides an advantage for large force production capacity per gram of muscle tissue, but pennate-fibered muscles are less capable of performing mechanical work and power (Gans, 1982; Azizi et al., 2008).

There are four types of fiber pennation observed in mammal skeletal muscles: unipennate, bipennate, multipennate, and rarely circumpennate (Lieber, 2002). Unipennate muscles have fascicles oriented in a single plane at some angle relative to the muscle line of action. Pennation angles are relatively low for unipennate muscles ranging from 15° to 25° (Musculino, 2011). Bipennate muscles have fascicles oriented at some angle relative to the muscle line of action on both sides of a central tendon within the muscle belly that is continuous with its insertion, reminiscent of a bird feather (Lieber, 2002). Pennation angles of bipennate muscles are typically larger than those of unipennate muscles (e.g., 20–35°). Multipennate muscles have a central tendon that branches into two or more tendinous inscriptions that run longitudinally throughout the muscle belly with short muscle fibers arranged obliquely in between each division (Musculino, 2011). Pennation angles are observed to be relatively high for multipennate muscles and can range from 25° to 45° (Gans, 1982, Zajac, 1989, 1992). Multipennate muscles have short fascicles and large PCSA. The m. subscapularis, a scapular stabilizer muscle, is an example of a muscle that is almost universally multipennate in mammals, although pennation angles may be low depending on the taxa and it functional habits (e.g., climber vs. digger). Last, in circumpennate muscles, fibers are arranged radially and connected to all sides of the central tendon. The notable example of a circumpennate muscle is the m. subscapularis in human primates, which is a rotator cuff muscle.

Parallel-fibered muscles have long fascicles that may approximate the length of the muscle belly (Lieber, 2002). Typically, the fascicles are orientated at low angles (0–15°) to the force axis of the muscle (Zajac, 1989,92). The shape of parallel-fibered muscles can be divided into three categories: strap, fusiform, and fan-shaped (Gans, 1982). Fascicles that are arranged in parallel to the line of action provide the advantage of shortening ability (i.e., contractile excursion) and velocity of contraction, which is

proportional to muscle fascicle and/or fiber length. Generally, parallel-fibered muscles have a larger capacity for performing work and power than pennate-fibered muscles, but they are less capable of producing large force. Parallel muscles with long fascicles are thusly specialized for fast movements or extensive movements requiring a large ROM at the limb joints.

Complete measurements of muscle architectural properties include muscle moment arm length (r_m), muscle mass (MM), belly length (ML), fascicle length (L_F), pennation angle (θ), and PCSA. Specifically, PCSA is the most important architectural property, and it can be calculated with the following equation:

$$PCSA = (V/L_F) \times \cos \theta,$$

EQ.1

where V is muscle volume (in g/cm^3), L_F is mean fascicle length, and θ is mean pennation angle in degrees. While PCSA is typically larger in pennate-fibered muscles, it is important to recognize that parallel-fibered muscles with large mass can also have large PCSA due to the use of volume (mass and volume are related by density) in its calculation. Nonetheless, direct calculation of PCSA from measured linear geometric dimensions allows for estimation of several function capacities of muscles including isometric force (F_{max}), maximal joint torque (at a joint angle of ~90°), and instantaneous muscle power (P_{inst}). Several architectural indices (AI) also provide information on the functional capacities of muscles. The ratio of fascicle length to muscle length (L_F/ML) predicts shortening velocity ability. A L_F/ML close to 1.0 indicates large contractile excursion instead of force due to long fascicles. Another important ratio is fascicle length to muscle moment arm length (L_F/r_m). The smaller the ratio calculated, the greater the mechanical advantage (MA) of an MTU at a joint for large force output. In contrast, a L_F/r_m greater than 2–3 indicates greater joint excursion per change in muscle fascicle length. MTU with large L_F/r_m ratios can move joints and limbs through large RoM and are often associated with powerful proximal muscles (e.g., hip extensors).

Architectural properties are available for the forelimb muscles of *B. variegatus* (Olson et al., 2018). To summarize, beyond gross observations of rope-like muscles with long, thin morphology, sloths demonstrated a general proximal-to-distal increase in pennation, and the flexors of the forelimb are stronger than the extensors. Notably, muscles with the

largest PCSA and ability to apply the greatest amount of joint torque are those that act to retract the limb (shoulder flexors) and the carpal/digital flexors in the antebrachium, although large mass and PSCA of the m. brachioradialis (BCR) make it the strongest flexor of the elbow. No muscles of *B. variegatus* were found to have the capacity for high power or large joint torques; however, numerous muscles of the forelimb were observed to have the ability to rotate the joints rapidly by their relatively short muscle moment arms and long fascicles (Olson et al., 2018). Yet, the extrinsic muscles of the forelimb in *Bradypus* have parallel fiber architecture but several have long moment arms for large joint torque application, and with the exception of mainly the distal carpal/digital flexors and extensors, the majority of the intrinsic musculature is slow contracting with relatively long, parallel or unipennate fibers (Olson et al., 2018).

Perhaps the most interesting finding in the forelimb of *Bradypus* was that each major flexor/extensor muscle group displayed pairings of muscles with long or short fascicles relative to their muscle moments arms (Olson et al., 2018). This type of muscle gearing was interpreted as a means for sloths perform slow, controlled movements, and it matches functional expectations for flexor/extensor musculature that can provide propulsion during both SW and VC, in addition to roles in body support in either orientation. Collectively, the architectural properties quantified in the forelimbs of three-toed sloths agree with roles in propulsion by pulling the body forward following touchdown (i.e., grasp on) of the limb on the substrate as well as the overwhelming function of suspensory support. Similar muscle properties should be expected of the hindlimb musculature, which may have an even greater role in support during suspension, but also might be required to perform work and power for vertical climbing.

c. Muscle Fiber Type

Muscle force production also depends on intrinsic fiber contractile properties, which are in turn dependent on myosin heavy chain (MHC) expression. Therefore, specialization of muscle fibers is also reflective of their expression of MHC isoforms. And although the distribution of muscle fiber types and/or motor units (MU) is directed by the size and conduction velocity of their alpha motor neurons, the contractile tasks routinely performed by a muscle or muscle group has the ability to modify the muscle fiber contractile and/or metabolic properties (Kohn, 2014; Thomas et al., 2017;

Spainhower et al., 2018). This phenomenon is understood as functional adaptation. Indeed, Schiaffino and Reggiani (1996) found that functional behaviors are one of the main determining factors of the intrinsic properties of muscle fiber types.

Mammals may express four adult myosin fiber types in their skeletal muscles: MHC-1, 2A, 2X, and 2B (Bottinelli, 2001). Slow MHC-1 fibers are historically considered to be oxidative (aerobic), have low power, and are the slowest-contracting adult muscle fibers (Kohn et al., 2007, 2011). MHC-2A fibers are faster-contracting and produce higher and power than the slow MHC-1 isoform. Fast MHC-2A fibers can be highly oxidative in their metabolism despite having some glycolytic (anaerobic) enzymatic properties (Schiaffino and Reggiani, 1996) and have the lowest contractile velocity of the fast-contracting isoforms. When the MHC-2A isoform is expressed in mammalian muscle fibers, larger cross-sectional area (CSA) than MHC-1 fibers have been commonly observed (Kohn et al., 2007), hence the fast fiber types have the capacity to produce larger isometric force than slow MHC-1 fibers. However, findings in sloths (Spainhower et al., 2018) and primates (Sickles and Pinkstaff, 1981) indicate that the predominant myosin fiber type expressed is often the largest, and thus produces the largest magnitude of force regardless of MHC isoform expression. MHC-2X fibers contract faster than MHC-2A isoform fibers and data from domesticated mammals show that they produce a greater force and have power output than MHC-2A fibers (Kohn et al., 2007). These same studies indicate that fast MHC-2X fibers are moderately oxidative-glycolytic in their fiber type metabolism. Last, the MHC-2B isoform is the fastest contracting and generate the highest power of all myosin fiber types. Fast MHC-2B fibers are historically shown to be the most glycolytic in their metabolism and have low fatigue resistance (Kohn et al., 2007). Large distributions of fast MHC-2B fibers are most typically expressed in limbs of rodents and lagomorphs (Schiaffino and Reggiani, 1996), as well as in the limbs of marsupials. Small mammals have a large surface area to volume ratio (SA: V) and must have muscles high intrinsic power to provide heat as major factor in their thermoregulatory strategy (Clarke and Rothery, 2007).

MHC fiber type and metabolic properties are available for sloths. A landmark study by Spainhower et al. (2018) found that both *C. hoffmanni* and *B. variegatus* only express slow MHC-1 and fast MHC-2A fibers in their forelimb musculature. Moreover, there is

predominant expression of slow MHC-1 fibers in all muscle functional groups, although a subtle slower-to-faster contracting change in fiber type distribution is observed along the length of the limbs. The distal forelimb musculature (e.g., carpal and digital flexors) are the only functional groups where the average proportion of slow MHC-1 fibers is exceeded by expression of the fast MHC-2A isoform (Spainhower et al., 2018). In the hindlimbs of sloths, there is also a relative increase in fast MHC-2A fibers in the digital flexors of both species, but slow MHC-1 fibers retain the largest percentage expression in all muscles studied (Spainhower et al., in revision). For example, *C. hoffmanni* and *B. variegatus* express similar large proportions of slow MHC-1 fibers in their hip flexors suggesting that the functional role of joint stability (i.e., anti-gravity muscles) of this muscle group is common to both species (Spainhower et al., in revision). Slow-contracting muscles are important to controlling acceleration of the CoM (i.e., minimizing destabilization of the body), which is related to the slow, deliberate locomotion of sloths (Nyakatura and Andrada, 2013). Specific examples include the shoulder flexors mm. pectoralis superficialis and deltoideus which are ~70% slow in their MHC fiber type distribution as are the elbow flexors/extensors, although large m. brachioradialis is the strongest elbow flexor and has a 95% expression of the slow MHC-1 isoform in *B. variegatus (Spainhower et al., 2018)*. The extremely slow-contracting BCR in *B. variegatus* is perhaps the best example of a muscle that emphasizes force while minimizing shortening velocity and these contractile features are generally reflective of sloth forelimbs (Olson et al., 2018).

Sloth limbs and those of primates, which have share overlapping ecological and behavioral preferences, are also extraordinarily similar in their myosin fiber type composition. For example, the fore- and hindlimbs of the slow loris (*Nycticebus coucang*), overall, have a similar expression of slow-contracting muscle fiber types (identified as Type I and Type IIA) (Sickles and Pinkstaff, 1981a, b). Two- and three-toed sloths, as well as *N. coucang*, also lack expression of the fast MHC-2X and -2B isoforms and these findings are notably suggestive of parallel evolution of slower contracting fiber phenotypes in mammalian taxa that exhibit obligatory suspensory behaviors or those that require grasping/clinging during vertical climbing. Strong, slow-contracting muscle fibers may therefore be a functional requirement for suspensory

habits. Sustained activations of numerous limb flexor muscles (see below) are expected to be necessary for the prolonged gripping/grasping behaviors in sloths and slow lorises.

d. Suspensory muscle function and mechanics

The initial understanding of muscle function during suspensory behaviors is primarily derived from foundational work with primates. Numerous studies in primate taxa have shown a relationship between muscle fiber type and EMG intensity during postural suspension and suspensory modes of locomotion (Jouffroy et al., 2004, and references therein; Jouffroy et al., 1999). The prevailing finding from these studies is that a near homogeneous expression of large, slow MHC-1 fibers is typical of a single belly (or muscle head) of each major extensor functional group (elbow, knee, and ankle extensors) in the limbs of primates sampled and has a postural function as an anti-gravity muscle. For example, m. vastus intermedius in a rhesus macaque is 90% slow contracting, a feature that notably correlates with its large fiber size and role in hindlimb joint stabilization (Jouffroy et al., 1999). During arboreal postural behaviors, these slow-contracting muscles show low-to-moderate levels of EMG activity while the fast-contracting muscles show low activity; however, all muscles show high-level activity during locomotion (Jouffroy et al., 1999; Jouffroy et al., 2004).

There is a total 89% fiber type distribution of the MHC-1 isoform in the limb musculature of three-toed sloths (Spainhower et al., 2018, in revision). Similarly, an extremely large percentage expression of slow MHC-1 fibers among the hindlimb flexors (88%) and extensors (93%) of three-toed sloths also suggests that their hindlimb muscles may collectively play a majority anti-gravity role. Support for this hypothesis is exemplified by the results of a very recent study (Gorvet et al., 2020) that evaluated EMG activation in the forelimb muscles of *B. variegatus*. The four main findings are summarized as the following: (1) the lowest volumes of active muscle were recruited during suspensory hanging (SH), where the distal carpal/digital flexors consistently showed the lowest levels of EMG activity among all muscles sampled; (2) flexor muscle activations were long and most intense during suspensory walking (SW) and found to be maximal for the elbow flexors and smallest for the carpal/digital flexors in forelimb; (3) EMG onset of the elbow and carpal/digital extensors occurred near mid-stance and either showed bi-phasic contact/swing activations or remained active through early swing

during suspensory walking, and showed greater relative activations during vertical climbing (VC); and (4) small, fast MHC-2A fibers were recruited at low intensities of activation during SH, whereas large, slow MHC-1 fibers were recruited at large intensities of activation during SW and VC.

The outcomes recounted from the analysis by Gorvet et al. (2020) is further suggestive of two major specializations to the tensile limb system of sloths. First, as previously hypothesized (Mendel, 1981b, 1985), largely passive weight-bearing in sloths is possible due to the presence of a (digital flexor) tendon suspensory apparatus that functionally analogous to that in upright ungulates (Mossor et al., in revision). Second, sloths appear to have neuromuscular modifications that can offset the cost of muscle contraction by selective recruitment of small, fast-contracting MU when less force is need for postural support that shifts to recruitment of large, slow contracting MU when greater force is needed for locomotor behaviors. Three-toed sloths may also have several forelimb muscles with super slow contraction velocities (i.e., V_{max}) based on their reported low mean EMG frequencies (Gorvet et al., 2020). These would be the slowest values for V_{max} yet to be reported in vertebrates.

Records of substrate reaction forces (SRF) are equally essential to understanding limb system function and suspensory mechanics in arboreal taxa. In contrast to the patterns typical of primates, which show hindlimb-biased body weight support as well as net propulsive impulse by the hindlimbs (Hanna et al., 2017), Granatosky and Schmitt (2017) showed that forelimbs of two-toed sloths (*C. didactylus*) are the main propulsion elements during SW, whereas the hindlimbs perform greater net braking. Beyond confirming the functional roles of fore- and hindlimb pairs during suspensory locomotion, three additional observations were made from the patterns of SRF in sloths: 1. Vertical SRF predominated indicating suspensory body-weight support (~70% vertical SRF) on arboreal substrates; 2. horizontal (fore-aft) forces were intermediate and vary in direction between the fore- and hindlimbs; and 3. medial forces on the substrate were appreciable, whereas lateral forces were negligible (Granatosky and Schmitt, 2017). Granatosky et al. (2018) also found that sloths do not shift their body weight between limb pairs during SW, thus maintaining the position of their COM evenly between the fore-and hindlimbs. Notably, these unusual mechanics of sloth locomotion are not fully

understood, but it was previously hypothesized (Granatosky et al., 2018; Gorvet et al., 2020) that co-activation of a forelimb flexor/adductor and hindlimb flexor/adductor during the contact phase of a suspensory walking stride might explain the patterns of SRF observed. It is also possible to co-contraction of epaxial/hypaxial musculature, in addition to specific limb muscles, would make the long axis of the body rigid when walking beneath branch to prevent shifting of the body weight (i.e., horizontal levering) and this prevents sloths from oscillating the substrate, which could lead to a fatal fall (fracturing the tree branch), and this is critical to fitness in sloths.

In sum, the previous findings (e.g., Nyakatura and Andrada, 2013; Granatosky and Schmitt, 2017; Granatosky et al., 2018; Gorvet et al., 2020) strongly suggest that locomotion in the limb system of tree sloths is entirely driven by muscle activation. Although, locomotor mechanics have yet to be studied in any species of *Bradypus*, and SRF are not available for climbing in sloths. During VC, both pairs of limbs are expected to have a propulsive and support function. This expectation is based on recent data from slow climbing lorids that use their forelimbs for propulsion (tensile loading) during the first half of a climbing stride and support (compressive loading) over the second half (Hanna et al., 2017). In fact, the contribution to vertical propulsion was relatively greater in the forelimbs of lorisids compared to their hindlimbs. Given the overall similarity in behavior between the slow loris (*N. coucang*) and sloths, it is likely that the hindlimbs of two- and three-toed forms also have an important anti-gravity role to play when grasping/clinging or climbing in an upright position.

Objectives and Hypotheses

This study aims to describe the myology of and quantify muscle architectural properties in the hindlimb of the brown-throated three-toed sloth (*Bradypus variegatus*). This work will build on historical studies of limb myology (Macalister, 1869; Humphrey, 1870; Mackintosh, 1875b) as well as recent novel investigations of muscle fiber architecture (Olson et al., 2018) and locomotor mechanics in sloths (Granatosky and Schmitt, 2017; Granatosky et al., 2018) to further interpret the functional roles of each limb pair. To this end, the contributions of the muscle mass and PCSA to force and torque application capacity will be used to further evaluate function in a tensile system in *Bradypus*. It is hypothesized that the muscle arrangements, mass distribution, and architectural

properties observed will be key anatomical correlates of functional roles in braking/support during SW and propulsion/support during VC.

Specifically, for sloth hindlimbs it is predicted that: (1) flexor group muscle masses will be greater than those of the extensor functional groups; (2) summed torques (i.e., strength) of the flexor musculature will be larger than those of the extensors at the hip, knee, and ankle joints; (3) m. sartorius, m. iliopsoas, and/or m. adductor longus will have large PCSA and MA at the hip joint for braking function during SW; (4) well-developed and strong knee flexors will have long muscle moment arms for the application of large medially-directed forces on the substrate to stabilize hindlimb support; and (5) hip extensors will have long fascicles, but appreciable muscle mass and moment arms for propulsion during vertical climbing. The expected results will substantially improve understanding of suspensory adaptations in sloth limbs; in particular, their ability to exert large force during slow contractions and minimize the metabolic cost of muscle contraction despite the lack of energy exchanges by pendulum (Nyakatura and Andrada, 2013) or elastic energy storage/recovery mechanisms (Biewener, 1998).